Science of the Total Environment 625 (2018) 1030–1045

Contents lists available at ScienceDirect

Science of the Total Environment

journal homepage: www.elsevier.com/locate/scitotenv

Predicting sediment yield and transport dynamics of a cold climate region watershed in changing climate

Narayan Kumar Shrestha, Junye Wang *

Athabasca River Basin Research Institute (ARBRI), Athabasca University, 1 University Drive, Athabasca, AB T9S 3A3, Canada

HIGHLIGHTS

- Climate change impact analysis on erosion and sediment transport of the Athabasca River Basin (ARB) using the SWAT model
- Future (mid- and late-century) climate data generated by three climate models for RCP 4.5 and 8.5 emission scenarios
- Impacts due to climate change are found to be region specific and land-use type dependent.
- Channel erosion and deposition were the dominant processes over hill slope erosion.
- Increment on soil erosion rate due to climate change is greater than reported soil formation rates.

GRAPHICAL ABSTRACT

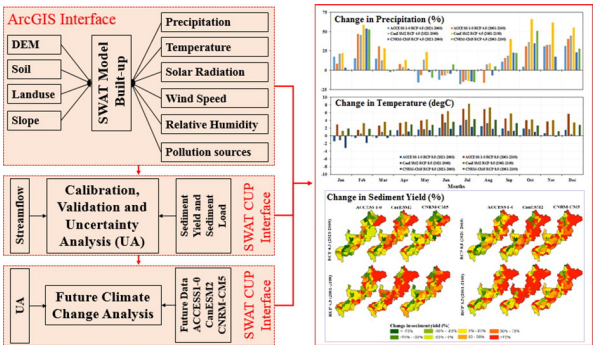

ARTICLE INFO

Article history:
Received 3 November 2017
Received in revised form 31 December 2017
Accepted 31 December 2017
Available online 5 January 2018

Keywords:
Cold climate regions
Climate change
Sediment yield and transport
Swat
Athabasca River basin

ABSTRACT

The effects of climate change on sediment yield and transport dynamics in cold climate regions are not well understood or reported. In this study, the Soil and Water Assessment Tool (SWAT) has been built-up, calibrated, and validated against streamflow and sediment load at several monitoring stations in a cold climate region watershed - the Athabasca River Basin (ARB) in Alberta, Canada. The model was then fed with bias-corrected spatial disaggregated high-resolution (~10 km) future climate data from three climate models for two emission scenarios (RCP 4.5 and 8.5), and two periods (mid- and end-century). Results show that channel erosion and deposition are the dominant processes over hill slope erosion in the basin. On average, a predicted warmer and wetter future climate has both synergetic and offsetting effects on sediment yield. Changes are sub-region specific and land-use type dependent, thus reflecting a marked spatial and temporal heterogeneity within the basin. Increases on sediment yield in future periods in the agricultural areas are up to 0.94 t/ha/yr, and are greater than reported soil formation rates in the region. Similarly, while substantial increases (by more than two fold) in the sediment load transport through the river reaches were obtained, the changes show both temporal and spatial variability, and are closely aligned with the trend of stream flows. We believe that availability of such models and knowledge of the effect of future climatic conditions would help water managers formulate appropriate scenarios to manage such basins in a holistic way. However, significant uncertainties in future sediment yield and transport, as a result of variations in climatic forcing of different climate models, need to be considered in any adaptation measures.

© 2018 Elsevier B.V. All rights reserved.

* Corresponding author.
E-mail address: junyew@athabascau.ca (J. Wang).

https://doi.org/10.1016/j.scitotenv.2017.12.347
0048-9697/© 2018 Elsevier B.V. All rights reserved.

1. Introduction

It is now evident that climate change is a real phenomenon (IPCC, 2014). Climate change induced hydrological altercations may pose a threat to water resources, can lead to excessive land degradation, and poses a threat to environmental sustainability of a river basin. Climate change affects erosion from upland catchments and the sediment transport in the river reaches in many ways (IPCC, 2007). Therefore, there is a pressing need to assess the impacts of a changing climate in the erosion and sediment transport dynamics of a river basin. Several studies have been conducted on this subject and widely reported in literature. In general, studies have shown that projected increases in temperature and projected increases or decreases in precipitation have resulted in contrasting situations. For instance, Adem et al. (2016) found a synergetic response of increases in temperature and precipitation on mean annual sediment yield in the Upper Gilgel Abay catchment, Blue Nile Basin, Ethiopia. However, Rodríguez-Blanco et al. (2016) found non-linear responses between changes in climatic variables and sediment concentrations in the Corbeira catchment, Spain due to complex interactions between climatic forcing, atmospheric carbon dioxide level, biomass, water yield (and streamflow), and soil detachment and transport dynamics. Similar observations have also been made by other researchers (Ficklin et al., 2013; Nunes et al., 2008; Serpa et al., 2015; Zabaleta et al., 2014). Interestingly, Serpa et al. (2015) observed two contrasting situations: decreases in erosion rates in a humid Mediterranean catchment with a permanent vegetation cover, and increases in erosion rates in a dry Mediterranean catchment with a perennial vegetation cover, which highlights the importance of vegetation cover on erosion rates. Based on the results on UK and European catchments, Dadson et al. (2010) also observed complex interactions between involved variables. However, they suggested that precipitation and land-cover would exert the strongest control over soil erosion dynamics. Similarly, Ficklin et al. (2013) highlighted the role of biomass growth as a result of a warmer temperature and its impact on surface runoff and erosion rates in an agricultural watershed in California, USA. In the Nam Ou basin, Lao PDR, Shrestha et al. (2013a) found significant uncertainty in sediment yield and flux as a result of variations in climate forcing of different models and stressed the need to consider the uncertainties in adaptation measures. Hence, it is evident that projected changes in erosion and sediment transport are region specific, and are the result of various underlying factors. Consequently, there is a need to assess the climate change impacts on erosion and sediment transport in new watersheds, including cold climate regions.

Cold climate regions service multiple ecosystem functions, such as climate regulation, water infiltration, and biodiversity conservation (AWC, 2011; Black, 1997). However, climate change and human activities, such as ever-increasing industrialization and a growing population, disturb these important ecosystems leading to severe land degradation. This has resulted in water quality impairments in receiving water bodies and have limited their ecological functions (Crabill et al., 1999). In order to understand and analyze such an interrelated and complex environment process, an integrated modelling framework that considers all terrestrial and aquatic ecosystems is needed (Argent et al., 2006). In such integrated modelling frameworks, erosion and soil transport modelling is essential because sediments provide surface area for contaminants to be adsorbed, and sediments can be a pathway for nutrient transfer from the river-bed to the water column and vise-versa (Ouattara et al., 2011; Shrestha et al., 2014; Shrestha et al., 2013b). In cold regions, such as the Athabasca River Basin (ARB) in Alberta, Canada, higher winter temperatures might convert non-erosive snowfall into erosive rainfall. This would melt permafrost, thereby increasing winter surface runoff, and leading to increased soil erosion from hill slopes and sediment transport through the reaches (IPCC, 2007; IPCC, 2014). Furthermore, exploration of the oil-sands is typical in the ARB. This can induce changes in the landscape of the basin. Less erodible forest would be changed into easily erodible, bare land patches. On such patches, increased erosive power of extreme rainfall would accelerate soil erosion by several fold. Similarly, in the lower regions of the ARB, where the river-bed slope is rather flat, deposition of large amounts of eroded sediment from upstream sub-basins would make navigation impossible, especially during low flow periods.

While there are a number of studies in which the ARB is assessed for climate change impacts, these studies have focused primarily on the variability and/or trends of stream flows. For instance, Eum et al. (2017) assessed impacts of climate change considering various hydrologic indicators (seasonal flows, timing and magnitude of maximum and minimum flows, and date and flow at spring freshet) at upper, middle and lower reaches of the ARB. Similarly, Leong and Donner (2015) evaluated impacts of climate change on annual flow, centroid of flow, and timing of spring runoff at a station downstream of oil-sands region of the ARB, including impacts on low-flow frequency. In a recent study, Shrestha et al. (2017) assessed green and blue water resources at different regions of the ARB. To the best of our knowledge, there has been little assessment of climate change impacts on sediment yield and transport dynamics in cold climate basins, in general and in the ARB in particular. Because of the consequences of land degradation, it is necessary to perform an assessment of climate change impacts on erosion and sediment transport in the ARB. As such, this study was carried out with the primary objective of quantifying the impacts of climate change on the sediment yield and transport dynamics in different spatial and temporal scales. For this, we calibrated and validated the Soil and Water Assessment Tool (SWAT) for this cold climate, snow dominated basin. Then, high resolution (~10 km) bias corrected, spatially disaggregated future climate data from three climate models for two emission scenarios (RCP 4.5 and 8.5) and for two future periods (mid- and end-century) was fed into the model. We believe that the results of this study can be translated for the holistic watershed management of the ARB as a whole, and is applicable to other cold climate regions as well.

2. Materials and methods

2.1. Study area

The Athabasca River Basin (ARB) is typical of cold climate basins. It lies in the centre of the province of Alberta in Canada and contributes significantly to the provincial economy by providing a continuous and dependable water supply to various industries and local communities (AWC, 2011). The river originates in the Columbia Icefields in Canada's Rocky Mountains and flows about 1500 km North-East, draining into Lake Athabasca in the north (Fig. 1). The catchment area of the ARB at the mouth is about 161,000 km^2. The river crosses through various urban centres in the process (AWC, 2011). Major industries in the basin include agriculture, forestry, pulp mills, coal mining, traditional oil and gas extraction, and oil-sands mining (AWC, 2013). The river receives point source pollution from waste water treatment plants in the urban centres, effluent from industries, and leachate from oil-sands tailing ponds (AWC, 2014), as well as non-point source pollution from agriculture.

Forest is the dominant land use type in the basin with almost 82% coverage. Of the different forest types, evergreen forest (FRSE, Table S1) has the highest proportion in all regions (Fig. S1) of the ARB. Relatively flat topography and a higher coverage of different types of forests (~90%) in the boreal plain region (Fig. S1) make this area least prone to erosion. However, the headwater region, with steep topography (slopes >20%, Fig. S2) and the highest percentage of barren land, make it most susceptible to erosion. Also, regions such as Prairie and Lesser Slave, which have the highest percentage of agriculture area, (~45% and ~19% respectively, Table S1), are prone to higher rates of erosion due to low or no vegetation cover in non-growing seasons.

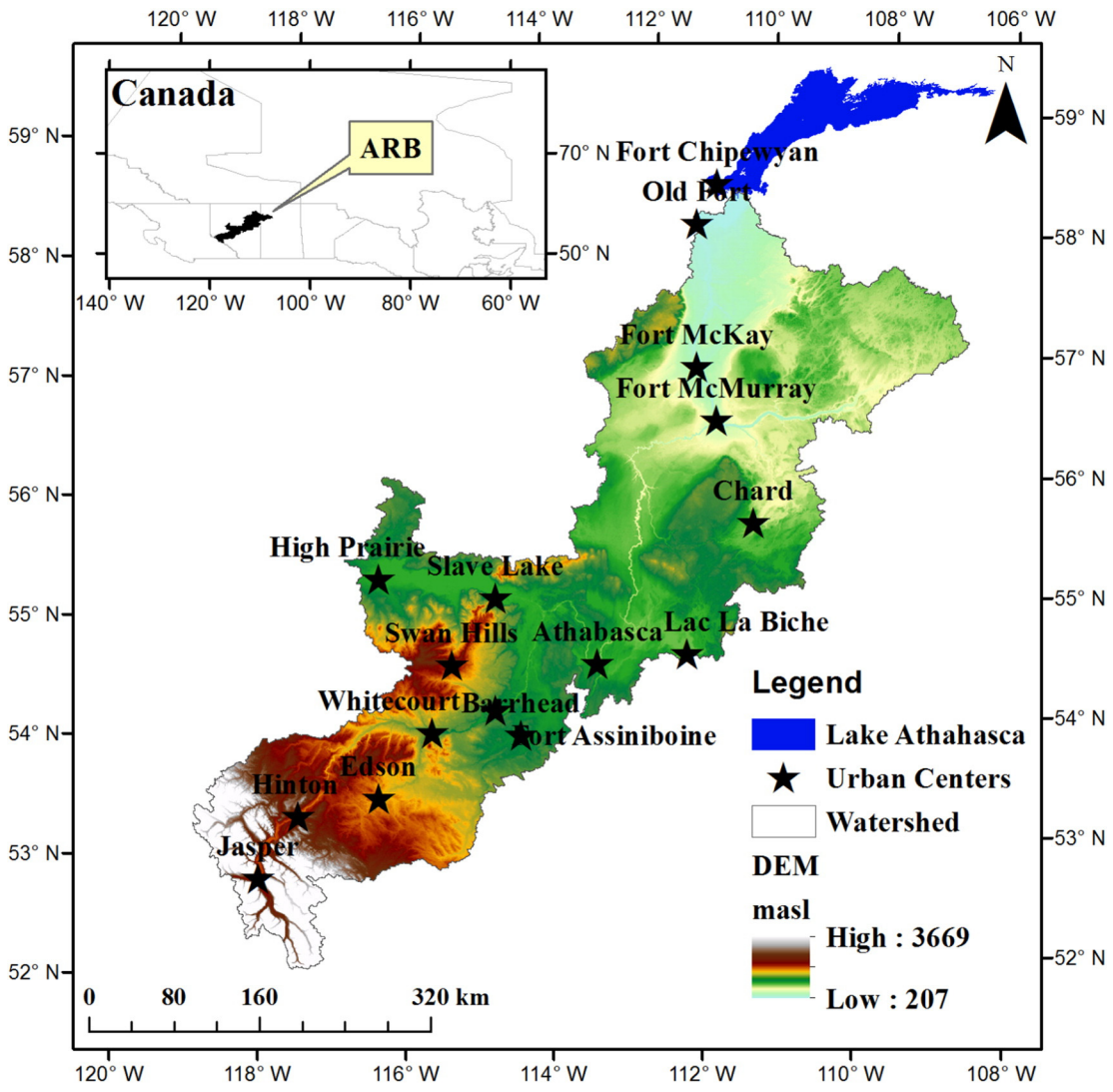

Fig. 1. Location of the basin with the Lake Athabasca, the outlet of the Athabasca River, digital elevation model (DEM) and urban centres.

2.2. The soil and water assessment model

The Soil and Water Assessment Tool (SWAT) is a semi-distributed hydrological simulator used for continuous, long term simulation of a variety of processes (Arnold et al., 1998). The simulator uses spatial datasets of elevation, land use and soil types along with several hydro-meteorological datasets, typically integrated using geographic information systems (Winchell et al., 2010). SWAT divides a watershed into sub-basins, which are further divided into Hydrological Response Units (HRUs), the latter being a unique combination of soil, land use and slope (Arnold et al., 2011). The hydrological compartment of SWAT considers precipitation, infiltration, deep aquifer, channel transmission and evapotranspiration losses, surface runoff, lateral and return flow for water balance calculations. SWAT uses the Modified Universal Soil Loss Equation to estimate soil erosion and sediment yield from each HRUs (Williams and Berndt, 1977):

$$sed' = 11.8\left(Q_{surf} * q_{peak} * area_{hru}\right)^{0.56} K_{USLE} * C_{USLE} * P_{USLE} * LS_{USLE} * CFRG \quad (1)$$

where, sed′ = sediment yield (metric tons); Q_{surf} = surface runoff (mm/ha); q_{surf} = peak runoff (m^3/s); $area_{hru}$ = HRU are (ha); K_{USLE} = soil erodibility factor (0.013 metric ton·m^2·ha/(m^3·metric ton cm)); C_{USLE} = cover and management factor (−); P_{USLE} = support practice factor (−); LS_{USLE} = topographic factor (−); CFRG = coarse fragment factor (−).

SWAT also accounts for the snow coverage effect on erosion (Neitsch et al., 2011):

$$sed = \frac{sed'}{\exp\left(\frac{3 * SNO}{25.4}\right)} \quad (2)$$

where, sed′ = sediment yield (metric tons), as in Eq. (1); SNO = water content of the snow cover (mm).

Sediment contribution from lateral and groundwater flows can also be considered. Once, sediments are in the stream, the sediment carrying capacity of the channel is determined as (Bagnold, 1977):

$$conc_{sed,ch,mx} = c_{sp}.v_{ch,pk}^{spexp} \quad (3)$$

where, $conc_{sed,ch,mx}$ = maximum sediment concentration that can be entertrained in the channel (tons/m^3); c_{sp} = a coefficient (−); spexp = an exponent parameter; $v_{ch,pk}$ = peak channel velocity (m/s) = $\frac{q_{ch,pk}}{A_{ch}}$ = $\frac{prf \cdot q_{ch}}{A_{ch}}$; prf = peak rate adjustment factor (−); A_{ch} = cross sectional area of the channel flow (m^2); q_{ch} = average channel flow (m^3/s).

The maximum carrying capacity is then compared against the initial sediment concentration at a reach ($conc_{sed,ch,i}$). If $conc_{sed,ch,i} > conc_{sed,ch,mx}$, then deposition prevails, otherwise, degradation prevails. The amount deposition or degradation is (Neitsch et al., 2011):

$$\begin{aligned} sed_{dep} &= \left(conc_{sed,ch,i} - conc_{sed,ch,mx}\right) \cdot V_{ch} \\ sed_{deg} &= \left(conc_{sed,ch,mx} - conc_{sed,ch,i}\right) \cdot V_{ch} \cdot K_{ch} \cdot C_{ch}. \end{aligned} \quad (4)$$

where, sed_{dep} = amount of sediment deposited (tons); sed_{deg} = amount of sediment degraded (tons); V_{ch} = volume of water (m^3); K_{ch} = channel erodibility factor (cm/ha/Pa); C_{ch} = channel cover factor.

After maintaining the sediment balance on the reach, the sediment concentration out of the reach is given as (Neitsch et al., 2011):

$$sed_{out} = sed_{ch} \frac{V_{out}}{Vch} \quad (5)$$

where, sed_{out} = sediment transported out of the reach (tons); sed_{ch} = sediment in the reach (tons); V_{out} = volume of water transported out of the reach (m^3); V_{ch} = volume of the water in the rach (m^3).

2.3. Model inputs and build-up

A 90 m × 90 m hole-filled digital elevation model (Jarvis et al., 2008) (Fig. 1), 1kmx1km Global Land Cover Characterization based land-use map (Loveland et al., 2000) (Fig. S1), and 1:1 million scale soil map (SLC, 2010) were the spatial datasets used in the model build-up. We are aware of potential benefits of finer resolution spatial datasets such as the DEM as it has been shown that finer spatial datasets tend to generate better hydrological (Teegavarapu et al., 2006) and soil erosion results (Zhang et al., 2008). However, some studies have also shown little effect of finer resolution DEMs up to 90 m (Reddy and Reddy, 2015). Owing to the spatial extent of the basin, the model used, and the need of long-term simulation in climate change impact studies, we believe that the resolution of spatial datasets used in the study would be appropriate. However, these spatial datasets could, preferably be replaced by finer ones. Then, a threshold drainage area of 200 km^2 was used to delineate sub-basins. Additional sub-basin outlets at major river confluences, and at stream flow and sediment monitoring stations, were defined. The process resulted in a total of 131 sub-basins. To define HRUs, a slope map was derived and divided into 4 classes (Fig. S2). Using a threshold of 10%, 5% and 10% for land use, soil and slope, respectively, a total of 1370 HRUs were obtained. Daily precipitation, maximum and minimum temperatures data at 73 stations recorded by (GoC, 2016), relative humidity, solar radiation, and wind speed data at 230 stations recorded by (CFSR, 2016) were fed into the model. To identify the point and non-point sources of pollution, we used a 30 m × 30 m crop inventory map (AAFC, 2013) and found 'Spring Wheat' and 'Barley' as the major crops grown in the basin. Accordingly, we assigned appropriate management operations (seedling and harvesting dates, and fertilizer rates) for these crops. While the forest is assumed to be growing at the start of the simulation, appropriate management operations for pasture (seedling and harvesting dates, and fertilizer rates), grassland and rangeland (grazing operation, daily biomass consumption, and manure production) were defined. Finally, annual constant point source data from 7 industrial effluents and 4 waste water treatment plants (AEP, 2016) were fed in to the model.

2.4. Model sensitivity analysis, calibration, validation and uncertainty analysis

The SWAT-CUP (Abbaspour et al., 2007) was used for the sensitivity, calibration and validation, and uncertainty analysis. The Nash Sutcliffe Efficiency – NSE (Nash and Sutcliffe, 1970) was used as the objective function. We chose the years 1980–1982 as a warm-up period, 1990–2005 for model calibration, and two different periods (1983–1989 and 2006–2013) for model validation. These periods were chosen systematically in order to include both drier and wetter periods, as determined by the Standardized Precipitation Index (SPI) (McKee et al., 1993). Refer Shrestha et al. (2017) to the SPI plots. This would ensure that the calibrated and validated model could simulate variables of interest satisfactorily in any (drier and wetter) future conditions (Daggupati et al., 2015). As erosion and sediment transport dynamics are hydrologically driven processes, simultaneous calibration of streamflow and sediment related parameters is required. Further, some parameters simultaneously affect the streamflow, erosion and sediment transport dynamics. As such, we selected 30 flow related (Table S2) and 10 sediment related parameters (Table 1) for sensitivity analysis. The model was calibrated using streamflow data (Environment-Canada, 2016) recorded at 35 stations (Fig. S3), and sediment data (AEP, 2016) recorded at 5 stations (Fig. 2). A proper calibration is assumed to be achieved when reasonable values of the selected goodness-of-fit statistics, and a good value of *p*- and *r*-statistics (ideal value is 1, and 0, respectively) is obtained (Table 2). The *p*-statistics reflect the percentage of observations bracketed by the 95% prediction uncertainty band, and the *r*-factor denotes the width of the band (Abbaspour et al., 2007). For the model performance evaluation, we chose Percentage of Bias (PBIAS), the NSE, and ratio of root-mean-squared error to standard deviation (RSR). Based on the range of values of these three selected goodness-of-fit statistics, we assigned a qualitative rating out of the four (Very Good, Good, Satisfactory and Unsatisfactory) suggested by Moriasi et al. (2007) to the model results.

2.5. Climate change data

Selection of suitable climate models to use for impact studies is not a straightforward task (Lutz et al., 2016). Different sources of uncertainties such as internal climatic variability, climatic model uncertainty and scenario uncertainty (Hawkins and Sutton, 2009) inherent in future climate projections necessitate the use of multiple data sources. Withstanding the obvious advantages of fine resolution climate data in process-based models, future climatic projections of Global Circulation Models (GCMs) are often downscaled and bias-corrected (Berg et al., 2012). As for the Western North America (WNA) region, Murdock et al. (2013) assessed accuracy of climatic projections (daily precipitation, maximum and minimum temperature) of all 26 GCMs involved in the Coupled Model Intercomparison Project (CMIP5) (Taylor et al., 2011), and ranked the top 12 GCMs for the WNA region. Using various downscaling methods, including the Bias-Correction/Spatial Disaggregation (BCSD), (Wood et al., 2004) using the ANUSPLIN data (Hutchinson et al., 2009), Murdock et al. (2013) prepared future climate data at 0.0833° × 0.0833° (~10 km × 10 km) spatial resolution. As such, we have used the same, bias corrected, spatially disaggregated daily precipitation, maximum and minimum temperature data from the top 3 GCMs (Centre National de Recherches Meteorologiques and Cerfaces – CNRM-CM5, Canadian Centre for Climate Modelling and Analysis – CanESM2, and Center for Australian Weather and Climate Research – ACCESS 1–0) out of the 12 recommended by (Murdock et al., 2013). Then, we downloaded and processed the datasets at 3306 grid points covering the ARB (Fig. S3) from the Pacific Climate Impact Consortium (PCIC) data portal. As for the other meteorological variables such as specific humidity (converted to relative humidity), solar radiation and wind speed, we used downscaled data (at a spatial resolution of 0.22° × 0.22°–25 km × 25 km) from the Canadian Center for Climate Modelling and Analysis (CCCMA), Regional Climate Model (RCM) - the CanRCM4 (Scinocca et al., 2015). We downloaded and processed the datasets at 273 grid points (Fig. S3). Furthermore, datasets corresponding to two IPCC AR5 emission scenarios - the RCP4.5 and the RCP 8.5 (IPCC, 2014) were considered. In order to quantify the climate change impacts in different time periods, a mid-century period (2040's) with a time frame of 2021–2060, and a late-century period (2080's) with a time frame of 2061–2100, are also considered. Finally, we divided the

Table 1
Sediment related parameters considered for the sensitivity analysis.

Name	Description	Unit	Min. value	Max. value	Default value
v__ADJ_PKR.bsn	Peak rate adjustment factor for sediment routing in the subbasin (tributary channels) - $prf_{tributary}$	–	0	2	1
v__PRF_BSN.bsn	Peak rate adjustment factor for sediment routing in the main channel (prf_{main})	–	0	2	1
v__SPCON.bsn	Linear parameter for calculating the maximum amount of sediment that can be reentrained during channel sediment routing (c_{sp})	–	0.0001	0.01	0.0001
v__SPEXP.bsn	Exponent parameter for calculating sediment reentrained in channel sediment routing (spexp)	–	1	2[a]	1
v__CH_COV1.rte	Channel erodibility factor (Kch)	–	−0.05	0.6	0
v__CH_COV2.rte	Channel cover factor (Cch)	–	−0.001	1	0
v__CH_ERODMO.rte	Monthly channel erodability factor (Kch, monthly)	–	0	1	0
v__USLE_C.plant.dat	Minimum value of USLE C factor applicable to the land cover/plant	–	0.001	0.5	Plant[b]
v__USLE_P.mgt	USLE equation support practice	–	0	1	HRU[c]
r__USLE_K.sol	USLE equation soil erodibility (K) factor	0.013 metric ton·m^2·ha/(m^3·metric ton cm)	−10%	10%	Soil layer[d]

v = parameter value is replaced by given value; r = parameter value is multiplied by 1 ± a given value
[a] Maximum limit widened.
[b] Plant dependent.
[c] HRU dependent.
[d] Soil layer dependent (maximum value = 0.65 and minimum value 0).

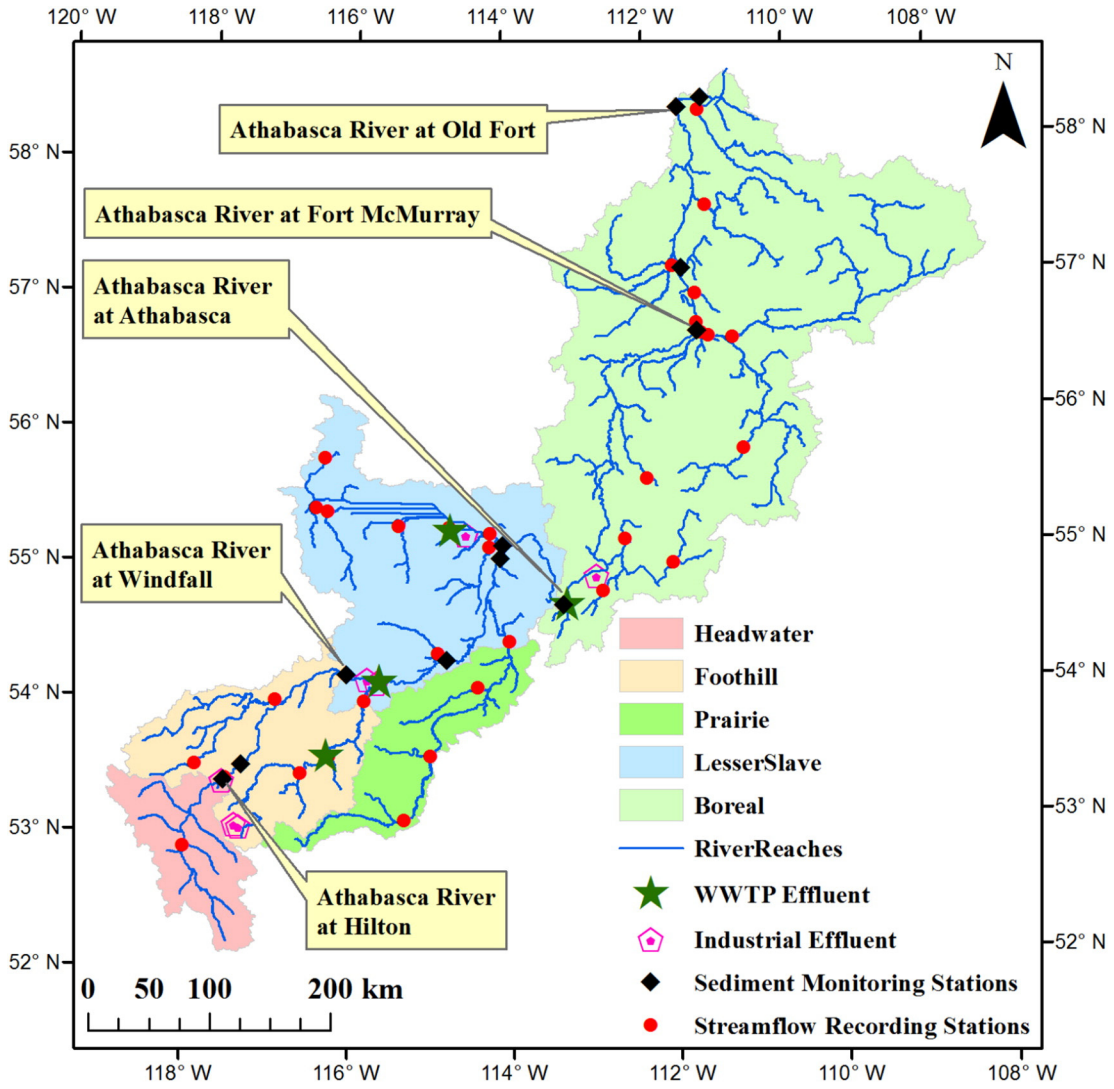

Fig. 2. The basin divisions (Headwater, Foothill, Prairie, Lesser Slave and Boreal) with streamflow recording, sediment monitoring, and point sources of pollution (industrial and waste water treatment plant) stations.

Table 2
Values of chosen goodness-of-fit statistics of sediment load simulation results in the calibration period with *p*- and *r*-statistics at five selected sediment monitoring stations.

Station	Figure	*n*	PBIAS	NSE	RSR	*p*-Stat	*r*-Stat
Headwater (Athabasca river at Hilton)	7 (a)	55	−6.5 (V)	0.42 (U)	0.76 (U)	0.47	1.15
Foothill (Athabasca river at Windfall)	7 (b)	59	59.8 (U)	−0.2 (U)	1.10 (U)	0.15	1.16
Lesser Slave (Athabasca River at Athabasca)	7 (c)	115	8.90 (V)	0.72 (V)	0.53 (V)	0.57	0.93
Boreal (Athabasca river at Fort McMurray)	7 (d)	115	6.80 (V)	0.75 (V)	0.50 (V)	0.37	0.84
Boreal (Athabasca river at Old Fort)	7 (e)	136	0.10 (V)	0.74 (V)	0.51 (V)	0.73	1.01

Statistics are calculated after transforming the sediment load in log (10-based) scale

n = number of observations, *p*-stat = percentage of observation captured by 95% predictive uncertainty band.
PBIAS = percentage of bias (%), *r*-stat = thickness of 95% predictive uncertainty band.
NSE = Nash-Sutfliffe Efficiency (−).
RSR = ratio of root-mean-squared-error to standard deviation of observations.

Qualitative rating for sediment, as per Moriasi et al. (2007)

V: Very Good Rating: PBIAS < 15%; 0.70 < NSE ≤ 1.00; 0.00 < RSR ≤ 0.55.
G: Good Rating: ±15% ≤ PBIAS ≤ ±30%; 0.60 < NSE ≤ 0.70; 0.55 < RSR ≤ 0.63.
S: Satisfactory Rating: ±30% ≤ PBIAS ≤ ±55%; 0.45 < NSE ≤ 0.60; 0.63 < RSR ≤ 0.71.
U: Unsatisfactory: PBIAS ≥ ±55%; NSE ≤ 0.45; RSR > 0.71.

ARB into five regions, namely – headwaters, foothills, prairie, Lesser Slave and boreal (Fig. 2) in order to quantify climate change impacts on a regional scale.

3. Results and discussion

The SWAT model is able to simulate the streamflow at various locations with varying degrees of accuracy (Fig. S4) as confirmed by the values of goodness-of-fit statistics (Table S3). However, we did not reproduce streamflow results in this paper and readers are thus referred to (Shrestha et al., 2017) for further details.

3.1. Parameter sensitivity

We refer to Shrestha et al. (2017) for details on sensitive parameters related to stream flows. Out of the sediment related parameters considered for sensitivity analysis, the channel cover factor (CH_COV2) and monthly channel erodibility factor (CH_ERODMO) were found to be the most sensitive parameters. The exponent parameter for calculating sediment carrying capacity in the channel (SPEXP) and peak rate adjustment factor for sediment routing in the tributary channel (ADJ_PKR) were found to be the third and fourth most sensitive parameters. Only one parameter related to erosion from upland processes, the land cover factor (USLE_C) for various plant types, was in the top 5 ranked sensitive parameters. This indicates that channel erosion is the dominant process in sediment transport in the ARB rather than upland erosion or sediment yield from sub-basins. This is expected, as the dominant land-use type in all regions of the ARB is forest (Table S1), and sediment yield from forest land-use is generally low. Furthermore, intense summer rainfall and high stream flow during spring due to snowmelt would generally cause substantial channel erosion. The sensitivity of the parameters obtained in this study is similar to other studies (Betrie et al., 2015; Vigiak et al., 2016) in similar watersheds.

3.2. Sediment yield from sub-basins

Fig. 3 shows spatial distribution of the annual average sediment yield from the delineated sub-basins of the ARB, and coefficient of

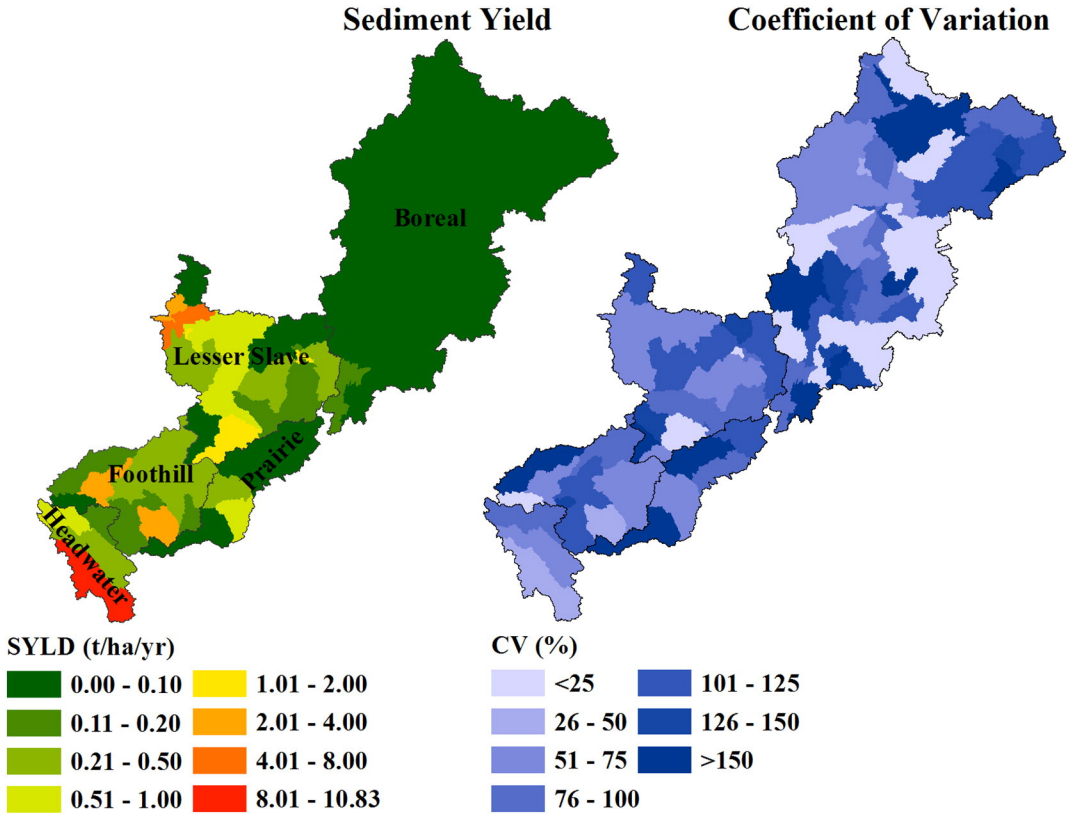

Fig. 3. Yearly averaged (left) and coefficient of variation (CV) sediment yield from sub-basins of the basin in base period (1983–2013).

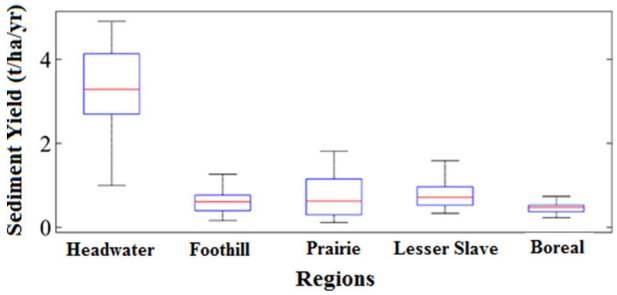

Fig. 4. Annual averaged sediment yield from different regions of the basin in base period (1983–2013).

variation during the base (1983–2005) period. The sub-basin average sediment yield of the ARB is found to be 0.4 t/ha/yr, which is within the range of values reported in the literature for this region. For instance, Bender et al. (2000) reported erosion rates for Alberta ranging from 0.05–46.8 t/ha/yr, and 0.05–2.6 t/ha/yr in the Oil-Sands regions of the basin. Similarly, Golder-Associates (1996) reported erosion rates in the US and Canada ranging from 0.16–27 t/ha/yr. As the ARB has flat topography (Fig. S2) and the majority of land-use type is forest (Table S1), it is quite natural that our average estimate falls into the lower end of the reported ranges in the literature. However, some sub-basins at the headwater region have sediment yield as high as 10 t/ha/yr (Fig. 3).

As expected, the headwater region is the main source of sediment with an average sediment yield of 3.23 t/ha/yr, as this region has steep topography and a higher percentage of bare-land. However, marked spatial heterogeneity in the sediment yield is evident in the basin (Fig. 3). Higher inter-annual variations of sediment yield, as indicated by the wider inter-quartile range of the box plot (Fig. 4) in the headwater region indicates that the sediment yield from this region of the ARB is sensitive to climatic forcing (e.g. precipitation) and land-use type. The scatter plot of annual precipitation and sediment yield (Fig. 5), and the slope of the linear trendline fitted between them, however, confirms that climatic forcing exerts greater control on erosion rates in the headwater region. It should be noted that the severity of instantaneous, extreme high rainfall is of higher significance than the total precipitation amount for the sediment yield from sub-basins.

At the foothills, while the slope is primarily <5% (Fig. S2), and forest is the dominant land-use type (Fig. S1, Table S1), the sediment yield (average: 0.6 t/ha/yr) reduced drastically in comparison to the headwater region. A narrower inter-annual variation (Fig. 4) and a fairly stable slope of the trendline (Fig. 5) indicates that sediment yield from the foothill region is mostly stable. While in the prairie and Lesser Slave regions, the average sediment yield is fairly comparable (0.78 and 0.8 t/ha/yr, respectively), some sub-basins of the regions have resulted in higher sediment yield as these regions have a substantial percentage of their area as agricultural land. The management operations carried out in the agricultural areas (e.g. plowing) would expose them to a higher risk of erosion. Further, agricultural areas have low vegetation cover during the cold season. As a result, although the majority of the area in these regions have a slope <5%, higher inter-annual variation in sediment yield (Fig. 4) also indicates higher susceptibility of the region to erosion. This is also reflected in the higher slope of the trendline (Fig. 5). At the boreal plains, as the topography is generally flat (slope < 5%), and >95% of its area is forest, the erosion potential is low, which is reflected in the sediment yield plot (Fig. 3). The narrowest box plot of inter-annual sediment yield (Fig. 4), and a very flat slope of the trendline also confirm this. The average sediment yield of the region is very low (average: 0.02 t/ha/yr).

As expected, the forest and rangeland have resulted in the lowest sediment yield, and the agricultural land has the highest yield (Fig. 6). This can be mainly related to land cover factors. The rangelands and forest consist of woody and/or herbaceous perennials, and top soil layers are barely exposed to the erosive effects of extreme rainfall, thereby leading to lower erosion. On the other hand, plants grown on the agricultural lands are annual ones, meaning that the top soil is exposed as bare (or low vegetation cover) for almost half of the year. Further, agricultural related operations such as plowing further loosen the top soil. Hence, erosive extreme rainfall would easily erode the top soil and these areas would yield higher amounts of sediment. Moreover, agricultural areas are often subjected to ephemeral gully erosion (Daggupati et al., 2014) albeit assisted by row cropping. In such a case, the concentration of channelized flow would lead to an even higher amount of erosion from agricultural areas. As we have seen, there is wider inter-quartile range of sediment yield from agriculture land, which also confirms the higher erosion potential of agricultural land. Our estimates of sediment yield from different land-use types are fairly comparable to the values reported in literature for similar watersheds. For instance, for forest land-use, Bender et al. (2000) reported citing Gray and Leiser (1982), US-EPA (1973), and US-EPA (1976), sediment yield of 0.078 t/ha/yr; Huang and Lo (2015) reported a range sediment yield value (0.02–0.07 t/ha/yr); and Rodríguez-Blanco et al. (2016) reported near zero (0.002 t/ha/yr) sediment yield. These values are fairly comparable to the median sediment yield (0.02 t/ha/yr) from the forest obtained in this study. Similarly, our estimate of mean sediment yield

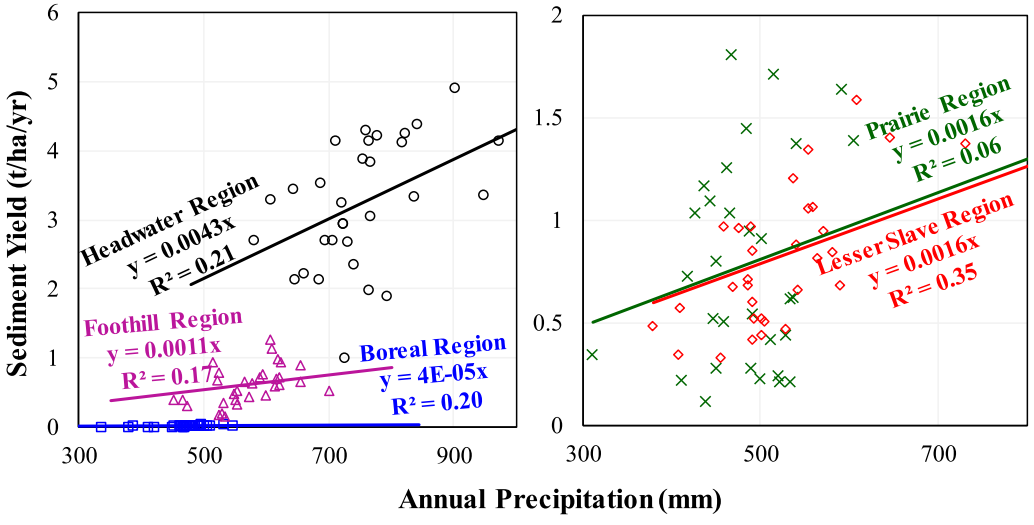

Fig. 5. Rate of sediment yield as function of total annual precipitation from different regions of the basin in base period (1983–2013).

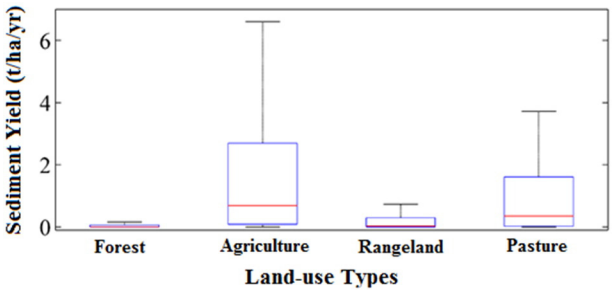

Fig. 6. Annual averaged sediment yield from different land-use types of the basin in base period (1983–2013).

(0.78 t/ha/yr) from rangeland is comparable to a value of 0.78 t/ha/yr by Bender et al. (2000) for grassland, and to a value of 1.01 t/ha/yr (Stephens et al., 1977) for woodland. However, our mean sediment yield estimate of 2.91 t/ha/yr from agricultural land seems to be a bit lower than most of the reported values; 15.6 t/ha/yr by Bender et al. (2000), 18.67 t/ha/yr by Stephens et al. (1977), 21.6–30 t/ha/yr by Huang and Lo (2015), and 3.09 t/ha/yr by Rodríguez-Blanco et al. (2016). While the sediment yield depends on various factors, a lower yield could be due to the relatively flat slope (<5%) in agricultural dominated areas of the ARB. Further, the mean annual precipitation in these regions is quite low (~500 mm), of which a significant proportion (~20%) is snowfall. However, we made an effort to increase the sediment yield at HRUs having agricultural areas as the land-use type, by increasing the related parameters to the upper end of the allowable range (e.g., C_{USLE} calibrated value = 0.45, maximum value = 0.5; and K_{USLE} fixed to its maximum value of 0.65, ADJ_PKR and PRF_BSN = 2). Similarly, the mean sediment yield from pasture is 1.53 t/ha/yr, which is also comparable to values reported in literature (0.78 t/ha/yr by

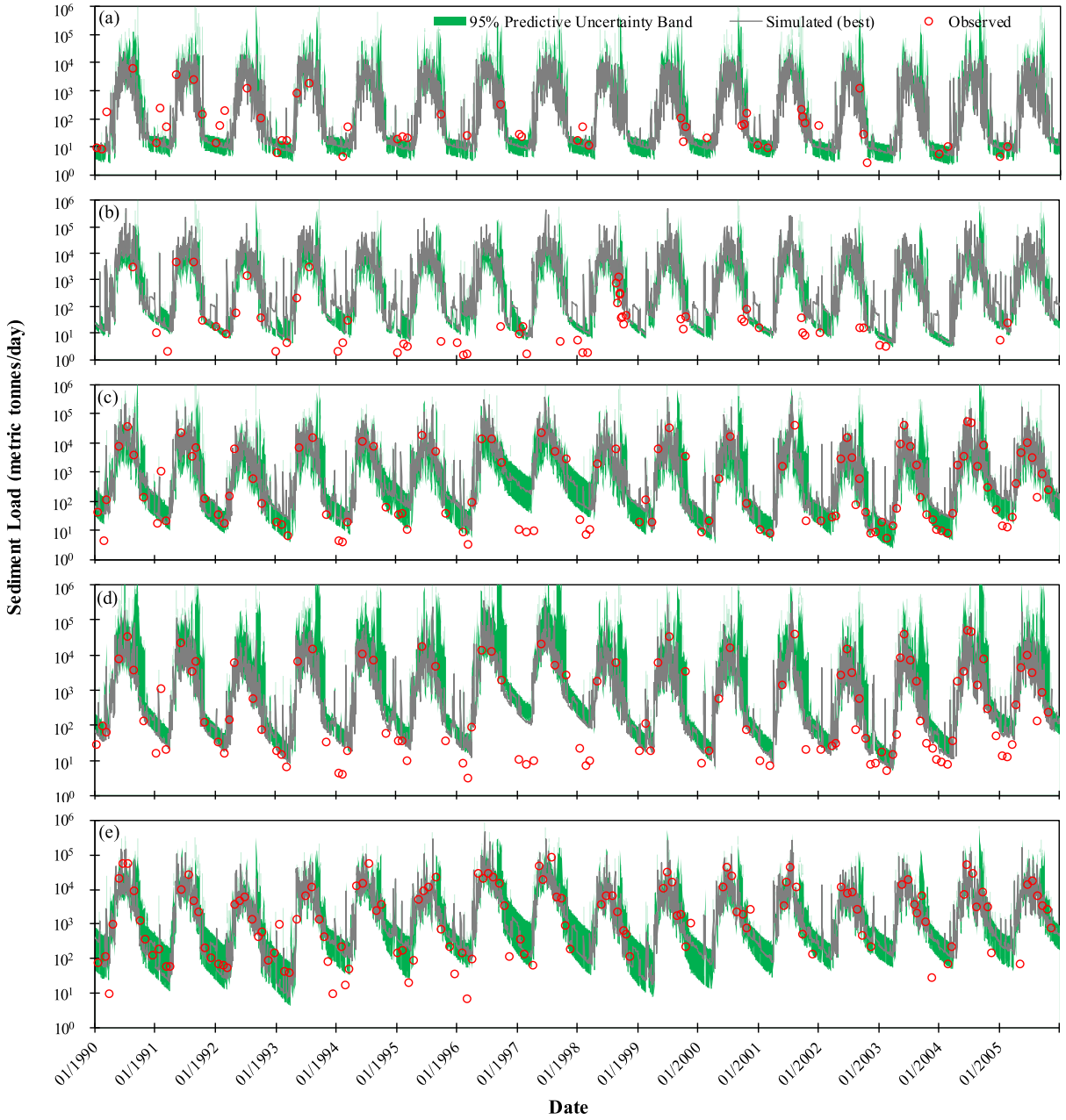

Fig. 7. Observed and simulated sediment load transported through (a) Headwater (at Hilton), (b) Foothill (at Windfall), (c) Lesser Slave (at Athabasca), (d) Boreal (at Fort McMurray), (e) Boreal (at Old Fort) in calibration period (1990–2005) with 95% total predictive uncertainty bands.

(Bender et al., 2000) and 4.33 t/ha/yr by Stephens et al. (1977), and higher than the estimate (0.005 t/ha/yr) of Rodríguez-Blanco et al. (2016). The optimized values for C_{USLE} for agriculture, forest, pasture and rangeland were 0.475, 0.009, 0.4505 and 0.005 respectively. Similarly, the optimized value for P_{USLE} was close to 1.0, and the optimized value for K_{USLE} for agriculture, forest, pasture and rangeland were 0.65, 0.05, 0.3 and 0.05 respectively. These parameters were tuned based on the initial estimate provided by AAFC (2002).

3.3. Sediment load transported through reaches

In general, the model is able to reproduce the trend in observations of sediment loads at all stations. Qualitative ratings of sediment load simulations indicate that the sediment load is simulated with a 'Very Good' accuracy (PBIAS < 15%, NSE > 0.7 and RSR < 0.55) at downstream stations (Fig. 7 c–e), while the sediment load is simulated with 'Satisfactory' accuracy in upstream stations (Fig. 7 a–b). Graphical plotting shows that, while the model tends to capture higher sediment load quite well, the lower sediment load has been slightly overestimated, especially at downstream stations. Such overestimation is typically observed in low flow periods (cold season). As the sediment yield from the upland catchments would be minimal, or even zero during such periods, the overestimation should thus be related to the sediment carrying capacity of the channel. Therefore, we purposefully lowered the values SPEXP and SPCON to their allowable minimum values and set CH_ERODMO value to zero. However, the lowered values of the parameters also lowered the higher sediment values and the model missed the high sediment loads. To overcome this problem, we increased the SPEXP beyond their allowable limit of 2.0, so as to get the desired effect of lowering sediment load during low flow periods and increasing sediment load during storm conditions. An illustration of the effect of SPEXP on the sediment carrying capacity of a channel for different sets of channel velocity ($V_{pk,ch}$) is shown in Fig. S5. It is evident that when $V_{pk,ch}$ is lower than 1.0 (low flow periods), the sediment carrying capacity decreases as the SPEXP increases. Conversely, when $V_{pk,ch}$ is >1.0 (storm conditions), the sediment carrying capacity increases as SPEXP increases. In the Bagnold's equation, which was mainly for non-cohesive particles, SPEXP ensures nonlinearities in the carrying capacity of a channel as velocities increase (for SPEXP ≠ 1.0). During low flow periods, cohesive sediment might only slightly erode, but when velocity increases, erosion of cohesive sediment might increase exponentially more than non-cohesive sediments. Hence, the use of SPEXP beyond

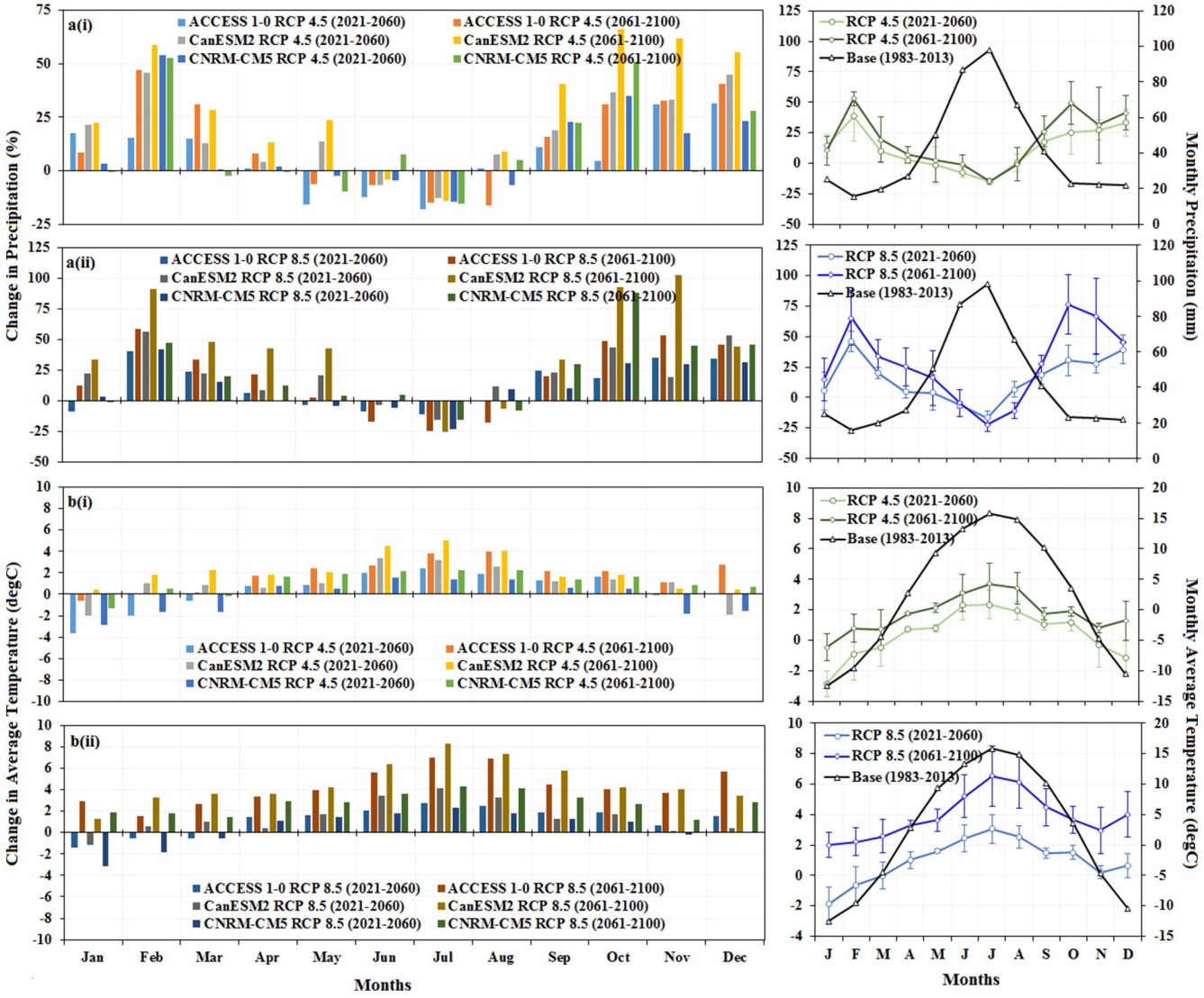
a(i)
ACCESS 1-0 RCP 4.5 (2021-2060)
ACCESS 1-0 RCP 4.5 (2061-2100)
CanESM2 RCP 4.5 (2021-2060)
CanESM2 RCP 4.5 (2061-2100)
CNRM-CM5 RCP 4.5 (2021-2060)
CNRM-CM5 RCP 4.5 (2061-2100)
RCP 4.5 (2021-2060)
RCP 4.5 (2061-2100)
Base (1983-2013)
a(ii)
ACCESS 1-0 RCP 8.5 (2021-2060)
ACCESS 1-0 RCP 8.5 (2061-2100)
CanESM2 RCP 8.5 (2021-2060)
CanESM2 RCP 8.5 (2061-2100)
CNRM-CM5 RCP 8.5 (2021-2060)
CNRM-CM5 RCP 8.5 (2061-2100)
RCP 8.5 (2021-2060)
RCP 8.5 (2061-2100)
b(i)
b(ii)
Change in Precipitation (%)
Monthly Precipitation (mm)
Change in Average Temperature (degC)
Monthly Average Temperature (degC)
Jan Feb Mar Apr May Jun Jul Aug Sep Oct Nov Dec
J F M A M J J A S O N D
Months

Fig. 8. (a) Percentage change in average monthly precipitation, (b) absolute change in average monthly air temperature over the basin between base and two future periods for two emission scenarios (i and ii).

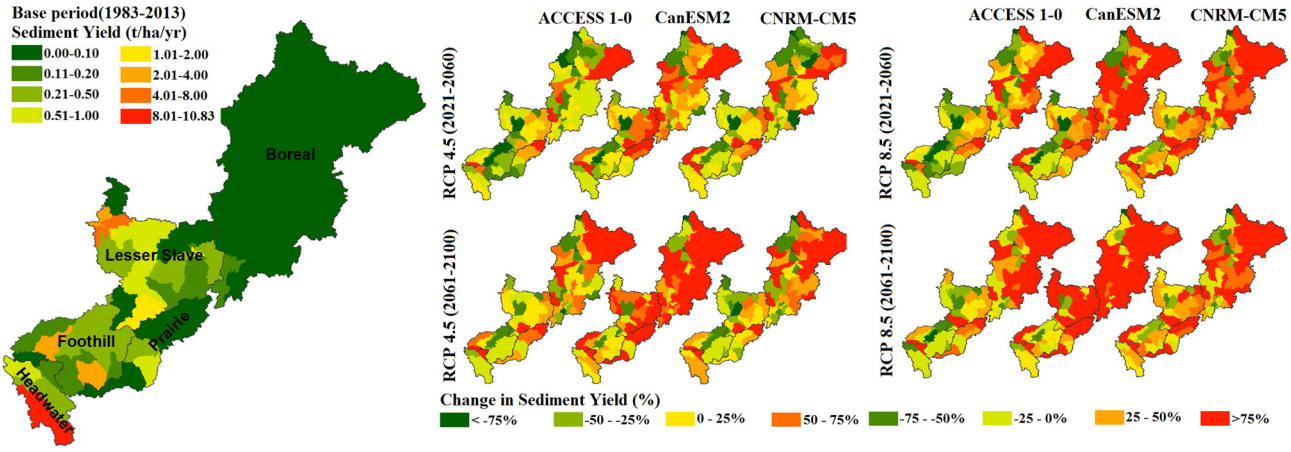

Fig. 9. Annual averaged changes in sediment yield (SYLD) from sub-basins of the basin in two future periods for two emission scenarios, relative to base period.

the maximum allowable limit might be justified. This issue indeed needs further investigation. The optimized values for the parameters; SPCON, SPEXP, CH_COV2, $CH\_ERODOMO_{Jan \rightarrow Mar \ \& \ Nov \rightarrow Dec}$, $CH\_ERODOMO_{Apr \rightarrow Oct}$ were 0.0002, 2.99, 0.975, 0.01 and 0.99, respectively.

3.4. Climate change impact

Basin-wide averaged monthly percentage and absolute changes of precipitation and temperature, respectively, in two future periods relative to the base period for two emission scenarios (Fig. 8) showed that weather in the ARB is projected to be warmer and wetter (except in Summer season), especially in the late-century period for the higher emission scenario. However, there are noticeable differences between the projections of different climate models. In general, CanESM2 based projections are relatively wetter and warmer than ACCESS 1–0 and CNRM-CM5 based projections. The mid-century mean annual temperature is projected to change by 0.4–2.0 °C, depending on the climatic models and emission scenarios. Further increases (1.7–5.2 °C) are expected in the late-century period. These increments are consistent with observations made by several studies, e.g. (Eum et al., 2017; Toth et al., 2006). Similarly, increases of 3–15% and 7–26% in annual average precipitation are expected in the mid-century and late-century periods, respectively relative to the base period. These increments are consistent (or slightly higher) with most of the reported values, e.g. (Eum et al., 2017; Toth et al., 2006). More extreme seasonal variations are expected in different regions of the ARB (Table S4). Except for the CanESM2 based projections, summer precipitation, which is of particular relevance to the erosion and sediment transport, is expected to decrease in all regions of the ARB. However, substantial increases in spring precipitation (up to 53%) and early spring freshet due to increases in spring temperature (up to 4.4 °C) would indicate that both soil erosion and sediment transport would increase in the future, especially in the spring season. Further, frequency analysis of extreme precipitation (daily precipitation >25 mm, Fig. S6) revealed that this events would become slightly more extreme, especially those corresponding to higher return periods (e.g. >100 years) and in the late-century period. Reflecting the trend of changes in precipitation, the streamflow, on average, is projected to increase in all seasons except at the foothills, prairie and Lesser Slave regions during the summer season (Table S5).

3.4.1. Sediment yield from different regions

The changes in the annual average sediment yield show marked spatial (Fig. 9) and temporal (Table 3, Table S6) heterogeneity. The changes are region, climatic model, future period, and emission scenario specific.

At the headwater region, the increase in annual sediment yield, on average, is highest (+11%) in the mid-century period for the higher emission scenario (Table 3), dominated by significant increases (up to 70%) in autumn period seasonal sediment yield (Table S6). This might be driven by higher occurrences of extreme precipitation for the mid-

Table 3
Percentage change in annual average in sediment yield in two future periods and for two emission scenarios, relative to base period (t/ha) in different regions of the basin.

Periods/regions	Climate model	Base period (1983–2013)	RCP 4.5 (2021–2060)	RCP 4.5 (2061–2100)	RCP 8.5 (2021–2060)	RCP 8.5 (2061–2100)
Headwater	ACCESS1-0	3.23	3.17 (−2%)	3.03 (−6%)	2.92 (−10%)	2.8 (−13%)
	CanESM2		3.18 (−1%)	3.59 (11%)	3.02 (−6%)	3.39 (5%)
	CNRM-CM5		3.82 (18%)	4.13 (28%)	3.44 (7%)	3.71 (15%)
	Mean (%)		3.39 (5%)	3.59 (11%)	3.13 (−3%)	3.3 (2%)
Foothill	ACCESS1-0	0.60	0.49 (−19%)	0.57 (−6%)	0.41 (−32%)	0.46 (−24%)
	CanESM2		0.56 (−7%)	0.73 (20%)	0.56 (−8%)	0.65 (7%)
	CNRM-CM5		0.59 (−3%)	0.56 (−8%)	0.58 (−4%)	0.69 (14%)
	Mean (%)		0.55 (−10%)	0.62 (2%)	0.51 (−15%)	0.6 (−1%)
Prairie	ACCESS1-0	0.78	0.62 (−20%)	0.73 (−6%)	0.65 (−16%)	0.64 (−18%)
	CanESM2		0.76 (−3%)	0.75 (−3%)	0.69 (−12%)	0.78 (0%)
	CNRM-CM5		0.69 (−12%)	0.61 (−21%)	0.62 (−20%)	0.82 (6%)
	Mean (%)		0.69 (−11%)	0.7 (−10%)	0.65 (−16%)	0.75 (−4%)
Lesser Slave	ACCESS1-0	0.80	0.73 (−9%)	0.9 (13%)	0.71 (−12%)	0.78 (−2%)
	CanESM2		1 (25%)	1.38 (71%)	0.99 (23%)	1.63 (103%)
	CNRM-CM5		0.83 (3%)	0.75 (−7%)	0.76 (−6%)	1.12 (39%)
	Mean (%)		0.85 (6%)	1.01 (26%)	0.82 (2%)	1.18 (47%)
Boreal	ACCESS1-0	0.02	0.01 (−31%)	0.01 (−14%)	0.01 (−19%)	0.02 (−2%)
	CanESM2		0.02 (−8%)	0.02 (41%)	0.02 (5%)	0.03 (70%)
	CNRM-CM5		0.01 (−28%)	0.01 (−21%)	0.01 (−25%)	0.02 (−5%)
	Mean (%)		0.01 (−22%)	0.02 (2%)	0.02 (−13%)	0.02 (21%)

century period (Fig. S6) and projected increases in autumn precipitation (Table S4). Note that the summer precipitation is expected to decrease up to 14% (Table S4). Further, projected increases in temperature seem to be favorable for plants as the number of temperature stress days (Table S7) is decreased, especially in the late-century period of the higher emission scenario. This would lead to increases in average annual biomass even though there are the fewest increases in the number of water stress days (Table S7)·This implies the combined effect of a net decrease in summer precipitation and in erosion in the headwater region is synergized by increased biomass growth, meaning increased leaf area index, thereby further reducing the erosive potential of extreme summer rainfall. A similar trend was also observed by various researchers, e.g. (Ficklin et al., 2013; Nunes et al., 2008). Consequently, summer sediment yield has been decreased by up to 36%. However, greater variability exists, as reported by the range (−36% to +22%) of changes in future summer sediment yield. In seasonal time scales, sediment yield from the headwater region showed marked heterogeneity. For instance, the sediment yield from the headwater region in the spring season, on average, has decreased (up to 8%, although CanESM2 based simulation in the late century period for higher emission scenario showed marked increase by 24%) even though increases in spring precipitation are predicted (up to 78%, Table S4). This might be due to earlier spring freshet as the mean air temperature is expected to increase in both winter (up to 3.7 °C) and spring (up to 3.8 °C) seasons. This will lead to a decreased snowpack. As for summer and autumn seasons, decreases and increases in precipitation, respectively, have been duly reflected in the sediment yield. Such temporal variability, as observed in this region, also highlights the dominating effect of seasonal variations in climatic forcing in the sediment yield. At the foothill region, while the severity of extreme precipitation is fairly comparable (to the base period) or has even been reduced, except for ACCESS 1–0 (in late century period and for lower emission scenario) and CNRM-CM5 (in late century period and for higher emission scenario) (Fig. S6), decreases in the annual sediment yield (up to 15%, Table 3) are thus

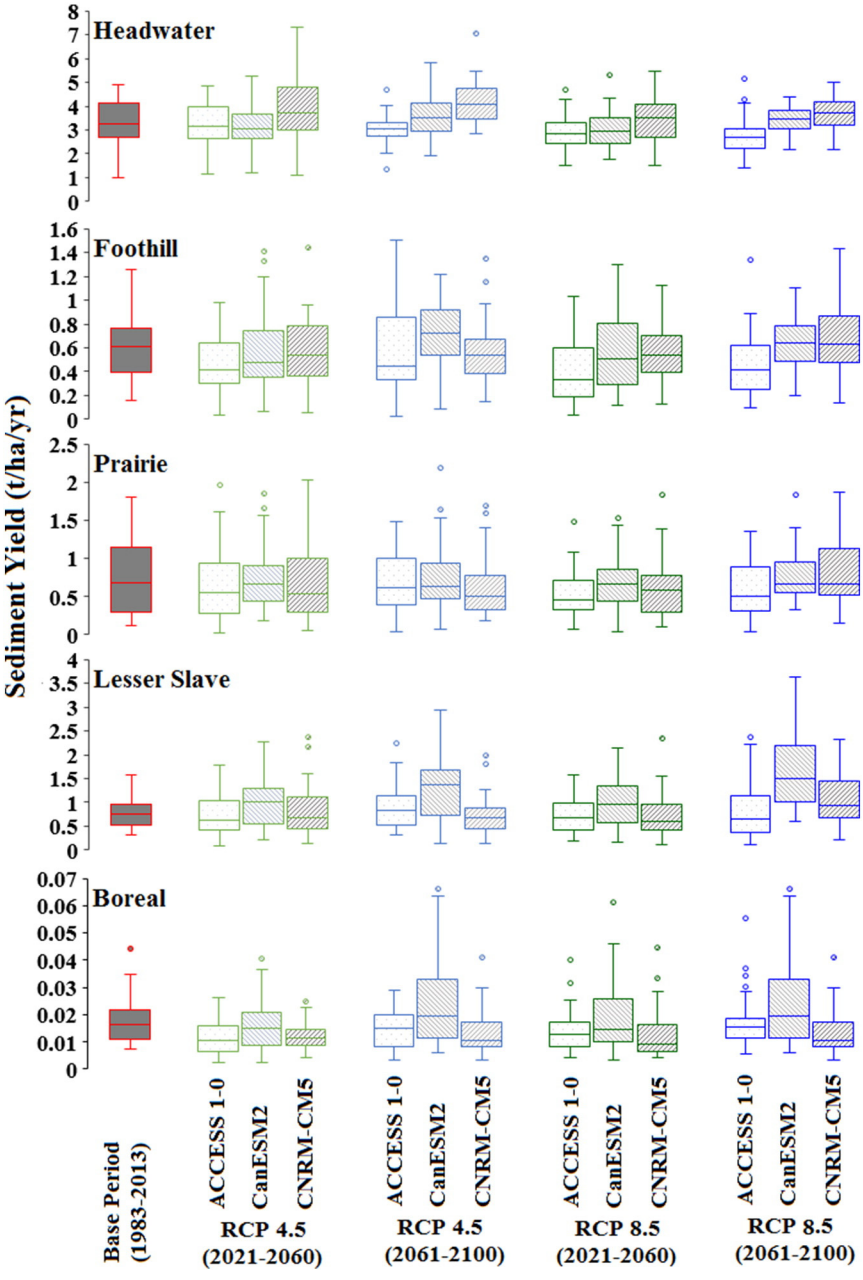

Fig. 10. Comparison of sediment yield from different regions of the basin in base and future periods for two emission scenarios.

evident. Decreases in summer sediment yield (up to 93%, Table S6) have mainly contributed to the overall decreases. Significant increases in mean winter air temperature (up to 5 °C, Table S4) in this region will lead to decreased snowpack for spring freshet, which would lower the surface runoff, causing marked decreases in the spring sediment yield despite of projected increase in spring precipitation. As observed in the foothill region, annual sediment yield in the prairie region also tends to decrease (Table 3). All three models' projections show significant increases (up to 5 °C, Table S4) in mean air temperature during winter season, resulting in decreased snowpack. Especially for regions such as prairie, where the percentage of agricultural land-use is the highest (Table S1), and agricultural areas during this period of time have no or low vegetation cover, even mild increases (10–69%) in winter precipitation have led to significant increases in winter sediment yield (>11 fold, Table S6). This further highlights the role of existing vegetation cover and precipitation dynamics on soil erosion. In the Lesser Slave region, projected increases in winter precipitation (Table S4) and earlier snow melt driven by projected increases in winter mean air temperatures are responsible for significant increases in winter sediment yield (up to 13 folds, Table S6). Projected changes in spring, summer and autumn rainfall are also reflected in corresponding sediment yields. Compared to the projections of other models, the CanESM2 driven future sediment yield at this region show the highest increases (up to 103%, Table 3), primarily caused by significant increases (up to 131%, Table S6) in spring sediment yield, which is driven by increases in spring precipitation (up to 49%, Table S4). In the boreal plain region, the reduced severity of extreme precipitation, especially for the lower emission scenario (Fig. S6), has led to decreased sediment yield for the emission scenario and in both periods (Table 3).

In general, a higher inter-quartile range of regional averaged sediment yield, especially for the late-century period and for the higher emission scenario (Fig. 10), closely aligns with the behavior of extreme precipitation events (Fig. S6). At regions where spring sediment yield dominates the annual sediment yield budget (e.g., foothills, prairie), earlier spring freshet tends to decrease sediment yield, albeit also aided by denser vegetation as indicated by an increased biomass yield (Table S7). However, at regions where summer sediment yield has a higher proportion of the annual sediment yield budget (e.g. headwater); changes in summer precipitation have been reflected in the sediment yield. Further, there exists significant variability in future sediment yields based on climatic projections of different model centres at different regions of the ARB. For example, at upstream regions (headwater and foothills), CNRM-CM5 based simulations show the highest sediment yield compared to two other model based simulations. However, at downstream regions (Lessee Slave and boreal plain), CanESM2 based simulation showed the highest sediment yield (Fig. 10).

3.4.2. Sediment yield from different land-use types

Similar to the region specific changes on future sediment yield, changes are also land-use specific (Fig. 11, Table 4). Agricultural areas show the highest sediment yield rate of 2.91 t/ha/yr in the base period, which is projected to increase further by 11–32% (Table 4), depending on the models used, the future time period and emission scenarios, even though summer precipitation is expected to decrease in future (Table S4). As major crops in the agriculture area are planted in mid or late spring and agricultural land during that period of time has lower vegetation coverage, early spring freshet (due to projected increases in winter and spring mean temperature) makes the agricultural land prone to a higher rate of erosion (Dadson et al., 2010; Serpa et al., 2015). It is possible that projected increases in winter and spring precipitation in regions having the highest proportion of agricultural area (the prairie and Lesser Slave regions) may have led to these increases. A similar trend was expected and observed for the pasture as they can also be considered as annual plants. In forest and rangeland, the sediment yield is expected to decrease in both emission scenarios and time periods. As the climate becomes wetter and warmer, a more rapid plant growth is expected in the future (Table S7), which will reduce surface runoff, thereby lowering the sediment yield. Further, for the higher emission scenario, increased CO_2 concentration will increase plant residues in the soil, thereby reducing the cover and management factor (C_{USLE}), as C_{USLE} is regulated as a function of plant residue in the SWAT model (Arnold et al., 2011). This will also lead to a decreased sediment yield. Further, it could be argued that increased mean air temperature for the late century period (Table S4) would increase evapotranspiration in forest dominated regions, like the boreal plain, and the decreased amount of soil moisture would allow a higher infiltration of precipitated water, resulting in further decreases in sediment yield. The results obtained in this study are consistent with the observations made by various researchers (Ficklin et al., 2013; Rodríguez-Blanco et al., 2016). However, the relative effect of different variables (temperature, precipitation and land-use) on the sediment yield are indeed different. Yet, changes in precipitation and land-use might outweigh others and could exert greater influence on sediment yield (Dadson et al., 2010).

3.4.3. Sediment load transported through reaches

While the impact of climate change on the sediment load through a river reach certainly depends on the sediment yield from its contributing upland sub-basins, it will evidently be more influenced by the change on streamflow (Adem et al., 2016; Shrestha et al., 2016) as channel erosion can be a dominant process in changing climate with more extreme precipitation. This was also the case in this study. In general,

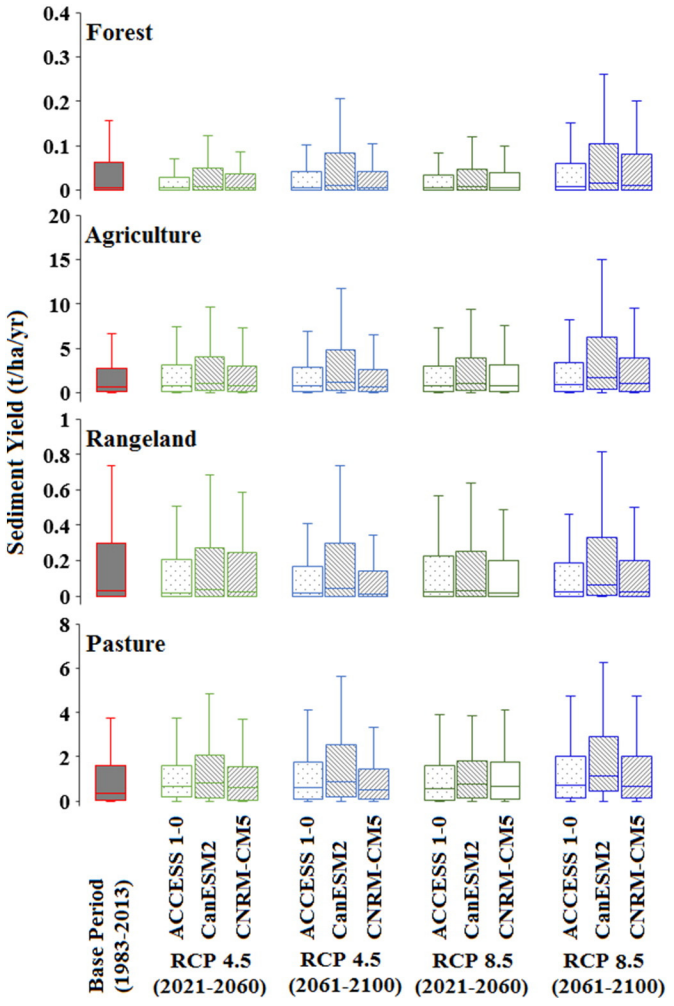

Fig. 11. Comparison of sediment yield from different land-use types of the basin in base and future periods for two emission scenarios.

Table 4
Percentage change in annual average sediment yield in two future periods and for two emission scenarios, relative to base period (t/ha) in different land-use types of the basin.

Periods/regions	Climate model	Base period (1983–2013)	RCP 4.5 (2021–2060)	RCP 4.5 (2061–2100)	RCP 8.5 (2021–2060)	RCP 8.5 (2061–2100)
Forest	ACCESS1-0	0.73	0.59 (−18%)	0.62 (−14%)	0.54 (−26%)	0.53 (−27%)
	CanESM2		0.6 (−17%)	0.75 (4%)	0.58 (−21%)	0.58 (−21%)
	CNRM-CM5		0.74 (2%)	0.81 (12%)	0.67 (−7%)	0.77 (6%)
	Mean (%)		0.64 (−12%)	0.73 (0%)	0.6 (−18%)	0.63 (−14%)
Agriculture	ACCESS1-0	2.91	2.82 (−3%)	3.33 (14%)	2.89 (−1%)	3.04 (4%)
	CanESM2		3.95 (35%)	5.18 (78%)	3.87 (33%)	3.87 (33%)
	CNRM-CM5		3.2 (10%)	3.05 (5%)	2.94 (1%)	4.35 (49%)
	Mean (%)		3.32 (14%)	3.85 (32%)	3.23 (11%)	3.75 (29%)
Rangeland	ACCESS1-0	0.78	0.55 (−29%)	0.65 (−17%)	0.58 (−26%)	0.53 (−31%)
	CanESM2		0.69 (−11%)	0.7 (−10%)	0.63 (−20%)	0.63 (−20%)
	CNRM-CM5		0.64 (−18%)	0.54 (−30%)	0.57 (−27%)	0.72 (−8%)
	Mean (%)		0.63 (−20%)	0.63 (−19%)	0.59 (−24%)	0.63 (−20%)
Pasture	ACCESS1-0	1.53	1.36 (−11%)	1.54 (0%)	1.44 (−6%)	1.45 (−5%)
	CanESM2		1.73 (13%)	2.04 (34%)	1.67 (9%)	1.67 (9%)
	CNRM-CM5		1.49 (−2%)	1.46 (−5%)	1.41 (−8%)	1.75 (14%)
	Mean (%)		1.53 (0%)	1.68 (10%)	1.51 (−2%)	1.62 (6%)

the change in sediment load tends to follow the pattern of streamflow change (Table S5).

At Hilton (headwater region), even the slight increases in the annual average sediment yield (Table 3) have amplified the increases in sediment load (Table 5, Fig. 12a). This indicates that channel erosion is the dominant process over hill slope erosion in this region of the ARB with a steep topography. During spring and summer seasons, although a lower amount of sediment has been delivered to the stream (Table 3), significant increases in winter and summer temperature have led to early snow freshet, thereby increasing streamflow significantly (up to 120% in winter and up to 148% in spring, Table S5). These increases have led to higher channel peak velocity, thereby boosting the sediment carrying capacity of the channel (Eq. (3)), which has resulted in substantial increases in sediment load (Table S8). During autumn season, driven by increases in autumn precipitation (Table S4), sediment yield from upland sub-basins has increased (Table S6) along with the streamflow (Table S5), which led to a synergetic effect on increases on sediment load (Table S8). A similar behaviour was also observed by Adem et al. (2016) in one of the catchments of the Blue Nile basin, Ethiopia. Furthermore, there exists marked intra-model variability in sediment loads as simulated using different model centres' projected climatic data (Fig. 12a), which are more evident in spring and autumn seasons in the end-century period. At Windfall (foothill region, Fig. 12b), while a similar monthly pattern as observed at the upstream station in the headwater region, the increase in annual average sediment load is relatively low (20–38%, Table 5), mainly driven by decreases in regional sediment yield in spring and summer seasons (Table S8). At Athabasca (Lesser Slave region), a similar trend has also been observed while slightly higher increases in sediment load can be observed at two stations in the boreal region (33–61% at Fort McMurray, and 47–57% at Old Fort, Table 5).Despite expected decreases in sediment yield at boreal plain region (up to 22%, Table 3), increases on sediment load can be perceived as the propagation of sediment load increments from upper river reaches, especially during the mid-century period. At seasonal scales, although the sediment yield in winter and autumn seasons remained unchanged (Table S6), significant increases in streamflow (on average, 31% in winter and 25% on autumn), have led to significant increases in sediment load (Table S8). During summer season, despite significant decreases in sediment yield (39–77%, Table S6), the sediment load has, on average, increased at both stations of the boreal region. However, simulations based on ACCESS 1–0 climate projections showed decreases (up to 31%) in sediment load transported through Old Fort.

3.5. Implications

From the analysis, it is evident that the ARB, on average, will become wetter and warmer in the future. However, summer precipitation, which is of special significance to erosion, is expected to decrease. On one hand, warmer climatic conditions will lead to a denser vegetative

Table 5
Percentage change in annual average sediment load in two future periods and for two emission scenarios, relative to base period in different reaches/regions of the basin.

Periods/location of reach	Climate model	RCP 4.5 (2021–2060)	RCP 4.5 (2061–2100)	RCP 8.5 (2021–2060)	RCP 8.5 (2061–2100)
Headwater (Athabasca river at Hilton)	ACCESS1-0	135%	156%	138%	166%
	CanESM2	180%	231%	186%	246%
	CNRM-CM5	148%	175%	158%	211%
	Mean	154%	187%	161%	208%
Foothill (Athabasca river at Windfall)	ACCESS1-0	6%	17%	11%	9%
	CanESM2	32%	52%	34%	51%
	CNRM-CM5	21%	32%	27%	54%
	Mean	20%	34%	24%	38%
Lesser Slave (Athabasca river at Athabasca)	ACCESS1-0	1%	9%	11%	−1%
	CanESM2	44%	83%	38%	89%
	CNRM-CM5	22%	29%	25%	62%
	Mean	22%	40%	25%	50%
Boreal (Athabasca river at Fort McMurray)	ACCESS1-0	7%	12%	18%	3%
	CanESM2	58%	109%	59%	113%
	CNRM-CM5	35%	33%	30%	67%
	Mean	33%	51%	36%	61%
Boreal (Athabasca river at Old Fort)	ACCESS1-0	22%	15%	30%	6%
	CanESM2	67%	119%	87%	98%
	CNRM-CM5	51%	38%	43%	55%
	Mean	47%	57%	53%	53%

cover, which leads to a decrease in sediment yield from the sub-basins. On the other hand, it will accelerate early snow freshet, which leads to higher sediment yields, especially during spring season. Withstanding the future changes in extreme precipitation, as they have a disproportionate effect on erosion relative to the total precipitation (IPCC, 2007), it is hard to quantify which phenomena would exert a greater control on sediment yield dynamics. We found the effect to be region specific and land use type dependent. Furthermore, there exists marked variabilities in sediment yield when using three model centres' future climatic data. While the use of two emission scenarios (RCP 4.5 and 8.5) and a higher number of climatic projections (from three model centres) have definitely reduced the scenario and model uncertainties inherent in these projections (Hawkins and Sutton, 2009), caution should be used while using these results in decision making processes, as is also suggested by various researchers, e.g. (Shrestha et al., 2013a; Zabaleta et al., 2014).

While comparing the projected erosion rates with soil formation reported in the literature, it is apparent that the ARB needs proper watershed management planning with a view of controlling soil erosion rates, especially in the headwater region and agricultural areas. The increases

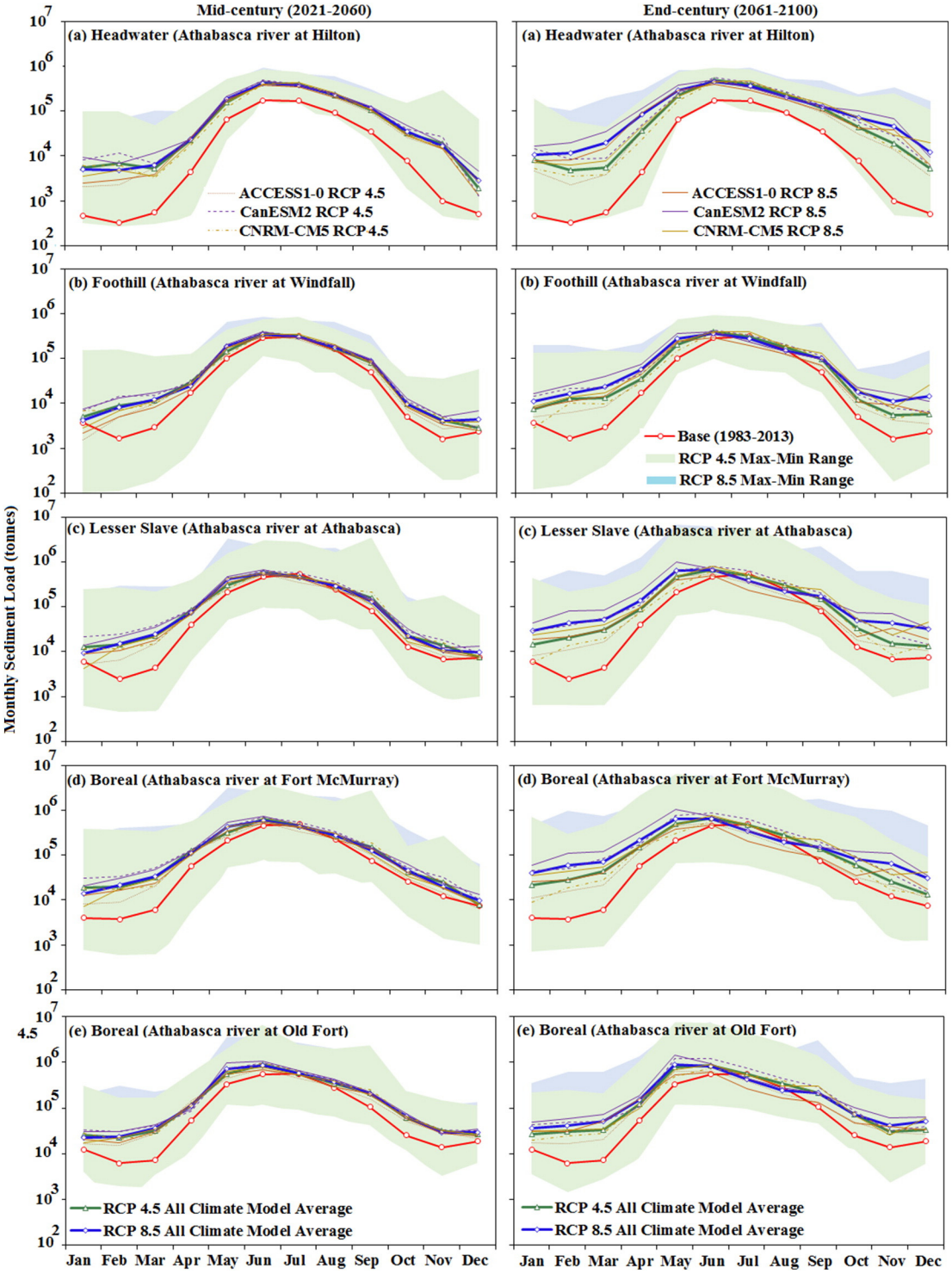
Mid-century (2021-2060)
End-century (2061-2100)
(a) Headwater (Athabasca river at Hilton)
(b) Foothill (Athabasca river at Windfall)
(c) Lesser Slave (Athabasca river at Athabasca)
(d) Boreal (Athabasca river at Fort McMurray)
(e) Boreal (Athabasca river at Old Fort)
Monthly Sediment Load (tonnes)
ACCESS1-0 RCP 4.5
CanESM2 RCP 4.5
CNRM-CM5 RCP 4.5
ACCESS1-0 RCP 8.5
CanESM2 RCP 8.5
CNRM-CM5 RCP 8.5
Base (1983-2013)
RCP 4.5 Max-Min Range
RCP 8.5 Max-Min Range
RCP 4.5 All Climate Model Average
RCP 8.5 All Climate Model Average
Jan Feb Mar Apr May Jun Jul Aug Sep Oct Nov Dec

Fig. 12. Comparison of monthly averaged percentage change in sediment load transported through different river reaches in base and future periods in two emission scenarios.

in annual average sediment yield from agricultural land are found to be up to 0.94 t/ha/yr. These increments are slightly higher than the soil formation rate in similar watersheds; e.g. 0.69–1.00 t/ha/yr (Alexander, 1988) and 0.569 t/ha/yr (Wakatsuki and Rasyidin, 1992). The loss of fertile top soil is indeed a serious concern in the agricultural industry. While decreases in average erosion rates from the dominant land-use types in the basin – the forest (up to 0.07 t/ha/yr), can be seen as the potential beneficiary of projected increases in temperature, although an increasing trend of land-use change especially driven by exploration of the multi-billion dollar oil-sands industry, would still pose some threats.

Further, the annual averaged sediment balance of the ARB in the base period indicated that the proportion of erosion to the total budget is rather low (8.27 Mt./year) when compared to that from channel erosion, especially from the upper reaches (117.90 Mt./year). Channel deposition at downstream reaches (111.23 Mt./year), lakes/reservoirs deposition (3.44 Mt./year), and sediment discharged at the basin outlet (5.05 Mt./year) complete the annual sediment balance. As observed, despite decreases in sediment yield rates in most of the regions of the ARB, the sediment load showed substantial increases, especially in the headwater region, indicating that channel erosion will be further exacerbated in the future, which will lead to further increases in channel sediment deposition in downstream reaches and in lakes/reservoirs. This would pose risks to navigation related activities at the downstream river reaches, especially during low flow periods and gully formation in upstream reaches. Further, increased sediment load to the lakes/reservoirs will not only decrease the capacity of the lakes/reservoirs, a problem also highlighted by Shrestha et al. (2016), but also increase nutrient delivery, which could lead to several environmental problems. Therefore, proper management efforts such as streambank stabilization, which is known to decrease channel erosion substantially (Vigiak et al., 2016), should be practiced in upstream reaches of the river.

4. Conclusions

As snowmelt dominates the runoff, streamflow dynamics and other related processes in cold climate regions, climate change induced alterations would result in more serious land degradation. So far, assessment of climate change impacts on erosion and sediment transport dynamics in cold climate regions, like the ARB, are scarce. Therefore, we built-up, calibrated and validated the SWAT model with special emphasis to snow related processes. Climate change effects on sediment yield and transport in the ARB at different spatial and temporal scales were quantified using high-resolution future climatic datasets.

Results show that climate change induced effects in sediment yield from upland sub-basins were region specific and land-use type dependent, indicating marked spatial and temporal heterogeneity. In cold climate regions, where annual sediment yield budget is dominated by spring season sediment yield, an earlier spring freshet due to projected increases in winter and spring temperatures led to decreased sediment yields. However, at regions where summer sediment yield dominated the annual sediment yield budget, such as in regions with steep topography, the projected decrease in summer precipitation also led to decreased sediment yield. As expected, the sediment yield from agricultural land was by far the highest (2.91 t/ha/yr) in the base period and would experience average annual increases up to 0.94 t/ha/yr. These increments are, in general, greater than reported soil formation rates in the region. As with the sediment yield, changes in the sediment load transport through reaches also show both temporal and spatial variability and have primarily followed the trend of future streamflow variability. Further, annual sediment estimates show that channel erosion and deposition were the dominant processes in hill slope erosion in the ARB. As these processes would be exacerbated in the future, suitable management practices such as streambank stabilization should be practiced in the ARB.

Acknowledgement

The authors would like to thank the Alberta Economic Development and Trade for the Campus Alberta Innovates Program Research Chair (no. RCP-12-001-BCAIP). We would also like to thank Dr. Xinzhong Du for processing the climate change data and Mr. Jim Sellers for proofreading.

Appendix A. Supplementary data

Supplementary data to this article can be found online at https://doi.org/10.1016/j.scitotenv.2017.12.347.

References

AAFC, 2002. RUSLEFAC: Revised Universal Soil Loss Equation for Application in Canada. A Handbook for Estimating Soil Loss from Water Erosion in Canada. Agriculture and Agri-Food Canada, Ontario, Canada.
AAFC, 2013. In: A-FuC, A.A. (Ed.), Annual Crop Inventory http://open.canada.ca/data/en/dataset/ba2645d5-4458-414d-b196-6303ac06c1c9.
Abbaspour, K.C., et al., 2007. Modelling hydrology and water quality in the pre-alpine/alpine Thur watershed using SWAT. J. Hydrol. 333 (2–4):413–430. https://doi.org/10.1016/j.jhydrol.2006.09.014.
Adem, A.A., et al., 2016. Climate change impact on sediment yield in the Upper Gilgel Abay Catchment, Blue Nile Basin, Ethiopia. In: Melesse, A.M., Abtew, W. (Eds.), Landscape Dynamics, Soils and Hydrological Processes in Varied Climates. Springer International Publishing, Cham:pp. 615–644 https://doi.org/10.1007/978-3-319-18787-7_28.
AEP, 2016. In: O., A. (Ed.), Surface Water Quality Data. Alberta Environment and Parks http://aep.alberta.ca/water/reports-data/surface-water-quality-data/default.aspx.
Alexander, E.B., 1988. Rates of soil formation: implication for soil-loss tolerance. Soil Sci. 145 (1).
Argent, R.M., et al., 2006. Comparing modelling frameworks - a workshop approach. Environ. Model. Softw. 21 (7):895–910. https://doi.org/10.1016/j.envsoft.2005.05.004.
Arnold, J.G., Srinivasan, R., Muttiah, R.S., Williams, J.R., 1998. Large area hydrologic modeling and assessment part I: model development. J. Am. Water Resour. Assoc. 34 (1), 73–89.
Arnold, J.G., et al., 2011. Soil and Water Assessment Tool Input/output File Documentation, Version 2009. 2011. Agrilife Blackland Research Center, Temple, Texas, p. 76502.
AWC, 2011. Athabasca Watershed Council - State of the Watershed Report: Phase 1. Athabasca Watershed Council, Hilton, Alberta.
AWC, 2013. State of the Watershed Report: Phase 3 - Water Quantity and Basic Water Quality in the Athabasca Watershed. Athabasca Watershed Council.
AWC, 2014. Athabasca State of the Watershed Assessment Phase 4: Organic Compounds in Surface Water and Sediments, and Trace Metals in Sediments. Athabasca Watershed Council.
Bagnold, R.A., 1977. Bed load transport by natural rivers. Water Resour. Res. 13 (2): 303–312. https://doi.org/10.1029/WR013i002p00303.
Bender, M.J., Sawatsky, L.F., Long, D., Anderson, P., 2000. Determining acceptable sediment yield for reclaimed mine sites. In: Haigh, M.J. (Ed.), Reclaimed Land: Erosion Control, Soil and Ecology. A.A. Balkema Publishers, Brookfield, VT, USA, pp. 37–49.
Berg, P., Feldmann, H., Panitz, H.J., 2012. Bias correction of high resolution regional climate model data. J. Hydrol. 448–449:80–92. https://doi.org/10.1016/j.jhydrol.2012.04.026.
Betrie, G.D., Deng, B., Wang, J., 2015. Integrated modelling of the Athabasca river basin using SWAT. 2015 Proceedings of Science and Technology Innovations. Athabasca University Press, Alberta, Canada, pp. 27–38.
Black, P.E., 1997. Watershed functions. J. Am. Water Resour. Assoc. 33 (1):1–11. https://doi.org/10.1111/j.1752-1688.1997.tb04077.x.
CFSR, 2016. In: G.W.D.f.S. (Ed.), Climate Forecast System Reanalysis http://globalweather.tamu.edu.
Crabill, C., Donald, R., Snelling, J., Foust, R., Southam, G., 1999. The impact of sediment fecal coliform reservoirs on seasonal water quality in Oak Creek, Arizona. Water Res. 33 (9):2163–2171. https://doi.org/10.1016/S0043-1354(98)00437-0.
Dadson, S., et al., 2010. Impacts of Climate Change on Erosion, Sediment Transport and Soil Carbon in the UK and Europe: Final Report. NERC/Centre for Ecology & Hydrology, UK.
Daggupati, P., Sheshukov, A.Y., Douglas-Mankin, K.R., 2014. Evaluating ephemeral gullies with a process-based topographic index model. Catena 113 (Supplement C): 177–186. https://doi.org/10.1016/j.catena.2013.10.005.
Daggupati, P., et al., 2015. A recommended calibration and validation strategy for hydrologic and water quality models. Trans. ASABE 58 (6):1705. https://doi.org/10.13031/trans.58.10712.
Environment-Canada, 2016. In: A.a (Ed.), Historical Hydrometric Data http://www.ec.gc.ca/rhc-wsc/.
Eum, H.-I., Dibike, Y., Prowse, T., 2017. Climate-induced alteration of hydrologic indicators in the Athabasca River basin, Alberta, Canada. J. Hydrol. 544:327–342. https://doi.org/10.1016/j.jhydrol.2016.11.034.
Ficklin, D.L., Luo, Y., Zhang, M., 2013. Climate change sensitivity assessment of streamflow and agricultural pollutant transport in California's Central Valley using Latin hypercube sampling. Hydrol. Process. 27 (18):2666–2675. https://doi.org/10.1002/hyp.9386.

GoC, 2016. In: GoC (Ed.), Environment and Natural Resources; Weather, Climate and Hazard http://climate.weather.gc.ca/.
Golder-Associates, 1996. Inventory of sediment yield from natural and disturbed surfaces. Technical Report No. 1. Syncrude Canada Ltd., Canada.
Gray, D.H., Leiser, A.T., 1982. Biotechnical Slope Protection and Erosion Control. Krieger Publishing Co. Inc., Florida, USA.
Hawkins, E., Sutton, R., 2009. The potential to narrow uncertainty in regional climate predictions. Bull. Am. Meteorol. Soc. 90 (8):1095–1107. https://doi.org/10.1175/2009BAMS2607.1.
Huang, C.T., Lo, F.K., 2015. Effects of land use change on sediment and water yields in Yang Ming Shan National Park, Taiwan. Environment 2 (1):32–42. https://doi.org/10.3390/environments2010032.
Hutchinson, M.F., et al., 2009. Development and testing of Canada-wide interpolated spatial models of daily minimum–maximum temperature and precipitation for 1961–2003. J. Appl. Meteorol. Climatol. 48 (4):725–741. https://doi.org/10.1175/2008JAMC1979.1.
IPCC, 2007. Climate Change 2007: Impacts, Adaptation and Vulnerability. Contribution of Working Group II to the Fourth Assessment Report of the Intergovernmental Panel on Climate Change. Cambridge University Press, Cambridge, U.K.
IPCC, 2014. Climate Change 2014: Synthesis Report. Contribution of Working Groups I, II and III to the Fifth Assessment Report of the Intergovernmental Panel on Climate Change, IPCC. IPCC.
Jarvis, A., Reuter, H.I., Nelson, A., Guevara, E., 2008. Hole-filled SRTM for the Globe Version 4. Available from the CGIAR-CSI SRTM 90m Database, CGIAR. http://srtm.csi.cgiar.org.
Leong, D.N.S., Donner, S.D., 2015. Climate change impacts on streamflow availability for the Athabasca Oil Sands. Clim. Chang. 133 (4):651–663. https://doi.org/10.1007/s10584-015-1479-y.
Loveland, T.R., et al., 2000. Development of a global land cover characteristics database and IGBP DISCover from 1 km AVHRR data. Int. J. Remote Sens. 21 (6–7):1303–1330. https://doi.org/10.1080/014311600210191.
Lutz, A.F., et al., 2016. Selecting representative climate models for climate change impact studies: an advanced envelope-based selection approach. Int. J. Climatol. 36 (12):3988–4005. https://doi.org/10.1002/joc.4608.
McKee, T.B., Doesken, N.J., Kleist, J., 1993. The Relationship of Drought Frequency and Duration to Time Scales, 8th Conference on Applied Climatology. American Meteorological Society, Anaheim, CA.
Moriasi, D.N., et al., 2007. Model evaluation guidelines for systematic quantification of accuracy in watershed simulations. Trans. ASABE 50 (3), 885–900.
Murdock, T.Q., Cannon, A.J., Sobie, S.R., 2013. Statistical downscaling of future climate projections, Pacific Climate Impacts Consortium (PCIC) (Victoria, British Columbia, Canada).
Nash, J.E., Sutcliffe, J.V., 1970. River flow forecasting through conceptual models part I—a discussion of principles. J. Hydrol. 10 (3):282–290. https://doi.org/10.1016/0022-1694(70)90255-6.
Neitsch, S.L., Arnold, J.G., Kiniry, J.R., Williams, J.R., 2011. Soil & Water Assessment Tool Theoretical Documentation, Version 2009. Grassland, Soil and Water Research Laboratory-Agricultural Research Service, Blackland Research Center-tTexas AgriLife Research.
Nunes, J.P., Seixas, J., Pacheco, N.R., 2008. Vulnerability of water resources, vegetation productivity and soil erosion to climate change in Mediterranean watersheds. Hydrol. Process. 22 (16):3115–3134. https://doi.org/10.1002/hyp.6897.
Ouattara, N.K., Passerat, J., Servais, P., 2011. Faecal contamination of water and sediment in the rivers of the Scheldt drainage network. Environ. Monit. Assess. 183 (1):243–257. https://doi.org/10.1007/s10661-011-1918-9.
Reddy, A.S., Reddy, M.J., 2015. Evaluating the influence of spatial resolutions of DEM on watershed runoff and sediment yield using SWAT. J. Earth Syst. Sci. 124 (7):1517–1529. https://doi.org/10.1007/s12040-015-0617-2.
Rodríguez-Blanco, L.M., et al., 2016. Potential impact of climate change on suspended sediment yield in NW Spain: a case study on the Corbeira catchment. Water 8 (10). https://doi.org/10.3390/w8100444.
Scinocca, J.F., et al., 2015. Coordinated global and regional climate modeling. J. Clim. 29 (1):17–35. https://doi.org/10.1175/JCLI-D-15-0161.1.
Serpa, D., et al., 2015. Impacts of climate and land use changes on the hydrological and erosion processes of two contrasting Mediterranean catchments. Sci. Total Environ. 538 (Supplement C):64–77. https://doi.org/10.1016/j.scitotenv.2015.08.033.
Shrestha, B., et al., 2013a. Impact of climate change on sediment yield in the Mekong River basin: a case study of the Nam Ou basin, Lao PDR. Hydrol. Earth Syst. Sci. 17 (1):1–20. https://doi.org/10.5194/hess-17-1-2013.
Shrestha, N.K., Leta, O.T., De Fraine, B., van Griensven, A., Bauwens, W., 2013b. OpenMI-based integrated sediment transport modelling of the river Zenne, Belgium. Environ. Model Softw. 47:193–206. https://doi.org/10.1016/j.envsoft.2013.05.004.
Shrestha, N.K., et al., 2014. Modelling *Escherichia coli* dynamics in the river Zenne (Belgium) using an OpenMI based integrated model. J. Hydroinf. 16 (2), 354–374.
Shrestha, B., Maskey, S., Babel, M.S., van Griensven, A., Uhlenbrook, S., 2016. Sediment related impacts of climate change and reservoir development in the Lower Mekong River basin: a case study of the Nam Ou Basin, Lao PDR. Clim. Chang.:1–15 https://doi.org/10.1007/s10584-016-1874-z.
Shrestha, N.K., Du, X., Wang, J., 2017. Assessing climate change impacts on fresh water resources of the Athabasca River basin, Canada. Sci. Total Environ. 601–602:425–440. https://doi.org/10.1016/j.scitotenv.2017.05.013.
SLC, 2010. In: A.aA.-fC (Ed.), Soil Landscapes of Canada Version 3.2 http://sis.agr.gc.ca/cansis/nsdb/slc/v3.2/index.html.
Stephens, H.V., Scholl, H.E., Gaffney, J.W., 1977. Use of the universal soil loss equation in wide-area soil loss surveys in Maryland. Soil Erosion: Prediction and Control. Soil Conservation Society of America, Iowa, USA, pp. 277–282.
Taylor, K.E., Stouffer, R.J., Meehl, G.A., 2011. An overview of CMIP5 and the experiment design. Bull. Am. Meteorol. Soc. 93 (4):485–498. https://doi.org/10.1175/BAMS-D-11-00094.1.
Teegavarapu, R., Viswanathan, C., Ormsbee, L., 2006. Effect of Digital Elevation Model (DEM) Resolution on the Hydrological and Water Quality Modeling. https://doi.org/10.1061/40856(200)216 (1–8 pp.).
Toth, B., Pietroniro, A., Conly, F.M., Kouwen, N., 2006. Modelling climate change impacts in the Peace and Athabasca catchment and delta: I—hydrological model application. Hydrol. Process. 20 (19):4197–4214. https://doi.org/10.1002/hyp.6426.
US-EPA, 1973. Methods for Identifying and Evaluating the Nature and Extent of Non-point Sources of Pollutants. US Environmental Protection Agency.
US-EPA, 1976. Erosion and sediment control. Surface Mining in the Eastern US. Volume I. Planning. Volume II. Design. US Environmental Protection Agency.
Vigiak, O., et al., 2016. Impact of current riparian land on sediment retention in the Danube River basin. Sustainability Water Qual. Ecol. 8:30–49. https://doi.org/10.1016/j.swaqe.2016.08.001.
Wakatsuki, T., Rasyidin, A., 1992. Rates of weathering and soil formation. Geoderma 52 (3):251–263. https://doi.org/10.1016/0016-7061(92)90040-E.
Williams, J.R., Berndt, H.D., 1977. Sediment yield prediction based on watershed hydrology. Trans. Am. Soc. Agric. Eng. 20 (6), 1100–1104.
Winchell, M., Srinivasan, R., Luzio, M.D., 2010. ArcSWAT Interface for SWAT2009 User's Guide, Soil and Water Research Laboratory-Agricultural Research Service (Blackland, Texas).
Wood, A.W., Leung, L.R., Sridhar, V., Lettenmaier, D.P., 2004. Hydrologic implications of dynamical and statistical approaches to downscaling climate model outputs. Clim. Chang. 62 (1):189–216. https://doi.org/10.1023/B:CLIM.0000013685.99609.9e.
Zabaleta, A., Meaurio, M., Ruiz, E., Antigüedad, I., 2014. Simulation climate change impact on runoff and sediment yield in a small watershed in the Basque Country, northern Spain. J. Environ. Qual. 43:235–245. https://doi.org/10.2134/jeq2012.0209.
Zhang, J.X., Chang, K.T., Wu, J.Q., 2008. Effects of DEM resolution and source on soil erosion modelling: a case study using the WEPP model. Int. J. Geogr. Inf. Sci. 22 (8):925–942. https://doi.org/10.1080/13658810701776817.